UNIVERSIDADE ESTADUAL PAULISTA
"JÚLIO DE MESQUITA FILHO"
Campus de Bauru

Faculdade de Ciências

POST-GRADUATE PROGRAM: SCIENCE AND TECHNOLOGY OF MATERIALS.

By: Dany Arnoldo Hernandez Baltodano

STRAIN RATE DEPENDENT BEHAVIOR OF COMPOSITE MATERIALS AND EPOXY.

Advisor: Dr. Marcelo Ornaghi Orlandi.

Bauru
March 2017.

DANY ARNOLDO HERNANDEZ BALTODANO

STRAIN RATE DEPENDENT BEHAVIOR OF COMPOSITE MATERIALS AND EPOXY.

Thesis submitted to Post-graduation program (POSMAT) from University of Sao Paulo ¨Julho de Mesquita Filho¨ (UNESP) Brazil in partial fulfillment of the requirement for the degree of Master in science and technology of materials.

Advisor: Prof. Dr. Marcelo Ornaghi Orlandi.

Bauru.

2017

Hernandez, Dany Arnoldo.
Strain rate dependent behavior of composite material and epoxy / Dany Arnoldo Hernandez, 2017
68 f.

Orientador: Marcelo Ornaghi Orlandi

Dissertação (Mestrado)–Universidade Estadual Paulista. Faculdade de Engenharia, Bauru, 2017

1. Composite materials. 2. Epoxy adhesive. 3. Scanning electron microscopy. I. Universidade Estadual Paulista. Faculdade de ciências. II. Título.

UNIVERSIDADE ESTADUAL PAULISTA

Câmpus de Bauru

Faculdade de Ciências

ATA DA DEFESA PÚBLICA DA DISSERTAÇÃO DE MESTRADO DE DANY ARNOLDO HERNÁNDEZ BALTODANO, DISCENTE DO PROGRAMA DE PÓS-GRADUAÇÃO EM CIÊNCIA E TECNOLOGIA DE MATERIAIS, DA FACULDADE DE CIÊNCIAS - CÂMPUS DE BAURU.

Aos 15 dias do mês de março do ano de 2017, às 14:00 horas, no(a) Instituto de Química de Araraquara, reuniu-se a Comissão Examinadora da Defesa Pública, composta pelos seguintes membros: Prof. Dr. MARCELO ORNAGHI ORLANDI - Orientador(a) do(a) Departamento de Físico-Química / Instituto de Química - UNESP - Araraquara, Prof. Dr. VLADIMIR GUILHERME HAACH do(a) Departamento de Engenharia de Estruturas / Escola de Engenharia de São Carlos Universidade de São Paulo, Prof. Dr. MARIO CILENSE do(a) Departamento de Físico-Química / Instituto de Química - UNESP - Araraquara, sob a presidência do primeiro, a fim de proceder a arguição pública da DISSERTAÇÃO DE MESTRADO de DANY ARNOLDO HERNÁNDEZ BALTODANO, intitulada **STRAIN RATE DEPENDENT BEHAVIOR OF COMPOSITE MATERIALS AND EPOXY.**. Após a exposição, o discente foi arguido oralmente pelos membros da Comissão Examinadora, tendo recebido o conceito final: APROVADO. Nada mais havendo, foi lavrada a presente ata, que após lida e aprovada, foi assinada pelos membros da Comissão Examinadora.

Prof. Dr. MARCELO ORNAGHI ORLANDI

Prof. Dr. VLADIMIR GUILHERME HAACH

Prof. Dr. MARIO CILENSE

This thesis is dedicated to my Father Pablo Emilio Hernández and to my Mother Celia Baltodano for doing of me who I am.

ACKNOWLEDGMENTS

I would first like to thank God for given me the opportunity to finish this master degree program. I would also like to thank to my parents, siblings and all my family members whose supported me at all time despite of the distance that separate us.

I would like to thank my advisor Dr. Marcelo Ornaghi Orlandi for all his support during the development of this research, thanks for have given to me confidence every time that I needed it, thank you for have accepted to be part of my professional development.

I would also like to thank Professor Carlos Alberto Soufen and professor Hamilton Jose de Melo for all their help, availability and comments during tensile test performance as well as the availability of the equipment of the mechanical engineering laboratory from UNESP-Bauru. Thanks are also addressed to microscopy technicians from UNESP IQ-Araraquara.

ABSTRACT

Considering the wide application range of composite materials for retrofitting civil engineering structures, it is found important to study the strain rate dependent behavior of both composite materials and some structural adhesive epoxies. Mechanical properties of Sikacarbodur S512 and adhesives bonding materials show different behavior when analyzed at different strain rates. Moreover, it was found that Sikacarbodur S512 is not a ductile material since it cannot sustain inelastic deformation because an elastic range governs its mechanical behavior. Epoxies adhesive do not have a significant plastic range; a viscoelastic range governs their main mechanical behavior under tensile loads. Sikacarbodur S512 analyses using scanning electron microscopy (SEM) shows that the fracture behavior is addressed by the interphase zone (contact zone between fiber and resin) which is affected by tensile stress concentration and cracks propagations. SEM analyses before and after tensile tests of both Sikadur 30 and Sikadur 330 shows that they have a continuous phase and a granular phase. In both resins, covalent bonds are broken, however sikadur 30 shows the most critical behavior. Sikadur 330 has better mechanical behavior under uniaxial tensile test than sikadur 30, and this better behavior is realized when their tensile strain to break and absorbed energy capacity are compared.

Keywords: Composite materials. Epoxy adhesive. Scanning electron microscopy.

RESUMO

Considerando as amplas aplicações de materiais compósitos para melhorar estruturas de obras em engenharia, é importante estudar a dependência do comportamento do material em função da velocidade de deformação aplicada aos materiais compósitos e aos epóxis adesivos. Propriedades mecânicas do material Sikacarbodur S512 e materiais adesivos mostram comportamentos diferentes quando analisados utilizando diferentes razões de deformação. Os resultados obtidos mostram que o Sikacarbodur S512 não é um material dúctil devido à ausência de capacidade de experimentar deformações inelásticas porque o domínio elástico domina seu comportamento mecânico. Os aditivos epóxis não têm domínio plástico considerável, e o intervalo visco elástico domina o seu comportamento mecânico sob forças de tração. As análises de microscopia eletrônica de varredura (MEV) das amostras de Sikacarbodur S512 mostram que o comportamento de fratura acontece na zona de interface (zona de contato entre as fibras e a resina) que é afetada pela concentração de tensões e propagações de trincas. As análises de MEV antes e depois dos testes de tração das amostras de Sikadur 30 e Sikadur 330 mostram que ambos os materiais possuem uma fase contínua e uma fase granular. Nas duas resinas as ligações covalentes são quebradas durante os testes embora o Sikadur 30 tem o comportamento mais crítico. O Sikadur 330 tem melhor comportamento mecânico do que o sikadur 30 e esse melhor comportamento é mais bem entendido quando compara-se suas deformações de ruptura em tensão e suas capacidades para absorver energia.

Palavras chave: Materiais compostos. Adesivos epóxis. Microscopia eletrônica de varredura.

LIST OF FIGURES

LIST OF TABLES

CONTENIDO

1 INTRODUCTION

Fiber Reinforced Polymer (FRP) systems for civil engineering applications are commonly designed and implemented by the companies. The cause for this lies in the unique nature of FRP laminates and the respective adhesives. There is an urgent need to standardize FRP composite materials, including adhesive, in a way, which promotes practicing civil engineers to design FRP composite for repairing bridge superstructures or building frames.

In order of understanding and standardize composites behavior, researchers´ have studied different composites materials regarding different cycles of loading at which composites materials are demanded. Shokrieh and Omidi [(1)] studied the tension behavior of unidirectional glass/epoxy composites under different strain rates from 0.001 to 100 s-1. They found that strength, stiffness, strain to failure and absorbed energy tend to increase with increasing strain rates. Moreover, they found that at quasi-static rate, damage is limited to small regions of the fracture surface with fiber pullout while at increasing rates the damage path covers the entire gauge section where extensive debonding between the fibers and the matrix was observed. Changes in failures modes from quasi-static to high dynamic loading cause an increase in energy absorption.

Hassein [(2)] studied how temperature affects the strength and the fatigue life of steel beams strengthened with externally bonded CFRP plates, using Sikacarbodur S512, sikadudur 30, a pre-impregnated laminate MTM 46/sts (24k) and MTM 46 epoxy resin. He determined material mechanical properties at different temperatures and then the interfacial stresses in epoxy resin between CFRP plate and steel beam. In CFRP tensile test (prepreg laminate), it was found that samples failed suddenly with not sign of any plastic deformation. However, the CFRP mechanical properties were assumed temperature independent for values of temperatures lower than matrix glass transition temperature (Tg). Moreover, tensile tests for sikadur 30 dogbone specimens were carried out at different temperatures to obtain Young modulus. And he observed that the sikadur 30 tensile strength is reduced and nonlinear stress-strain behavior is obtained when the temperatures becomes close and above Tg. Regarding sikadur 30 the work concluded that, glass transition temperatures (Tg) depends on the heating and loading rates, meaning that, sikadur 30 glass transition temperatures cannot be an exact value. Additionally two steel elements were bonded together using sikadur 30 and then a tensile load was applied

to perform pull-off tests. These tests indicated a dependence in the resin bond strength with temperature.

Some experimental tensile tests were carried out on double-lap shear specimens under static tensile loads at different temperatures (up to 60 °C) and time and temperatures dependency of the bonded shear were investigated. Moreover, bending tests were carried out on steel beams reinforced with CFRP plates at different temperatures to investigate effects of high temperatures on flexural capacity of CFRP strengthened beam[(2)] . Double-lap shear tensile static tests showed that the joint capacity decreases with increasing temperature, this is due to the reduction in strength and stiffness of the adhesive with temperature. In addition, the strain dropped suddenly in a very short time (less than 0.1 second) indicating abrupt debonding. Furthermore, he found that the strength of a bonded joint is dependent not only on temperature but also on time. Therefore, the properties of resin are time and temperature dependent even below Tg. The debonding static tests showed that beam flexural capacity decreases as temperature increases furthermore there was not increase in the stiffness of the reinforced beam because the elastic modulus of the CFRP was lower than that of the steel. However, the yield loads for the reinforced beams were increased when compare to the unstrengthen beam. In addition, it was found that strain along the plate increases and becomes nonlinear gradually with the load until the beam starts to yield, therefore, the plate starts to contribute to carrying more loads after beam has yielded.

Double-lap shear specimens and CFRP reinforced beams behavior at different cyclic loading levels and temperature were studied to investigate their fatigue life temperature dependence[(2)]. It was found that the fatigue life of the bonded joint decreases as either the load or the temperature increases. Increasing the load, intensify the stresses in the adhesive at the discontinuities thus; develop longer plastic zones at the adherents' ends. Furthermore, the fatigue life of the bonded joints is significantly decreased by increasing the temperature at the same applied load. Moreover, it was found that the fatigue failure of a bonded joint at high temperature could be avoided by increasing the CFRP plate length, because the average shear stress along the bonded joint and the plastic zone decrease with increasing the plate length. The stress analysis showed that the length of the plastic zones increase with both the applied load and the temperature. Furthermore, it showed that the fatigue life at the same applied load decreases significantly with increasing the temperature due to the reduction in the shear strength of the adhesive, thus the plastic zone increases. Bending fatigue tests in steel beams strengthened with CFRP plates at different cyclic loading ranges and temperature showed that

the debonding failure starts either at one of both plate ends and then propagate to the mid plate. In addition, the results show that the fatigue life of the CFRP reinforced beams decreases as temperature increases.

Most investigations explore the resin bond behavior and its capacity because it is typically the adhesive of the FRP composite system, that fails first. Michels, [3] et al., studied the influence of the curing condition (room temperature and accelerated curing) in glass transition temperature (Tg) of Sikadur 30, using Dynamic Mechanical Analysis (DMA) in the temperature range from -20 °C to 150 °C, regarding a constant heating rate of 2 °C/min and 0.5 °C/min. However just one sample was considered at heating rate of 0.5 °C/min. It was observed that glass transition temperature (Tg) is not a defined material property and it would vary depending on the definition considered for assessing it, besides that there were values of Tg in the region of 40 °C to 50 °C, as recommended values for civil structures designs.

McNutt [4] applied spring theory using Sikacarbodur, sikaWrap Hex 230, sikadur 30, sikadur 330 and LTC 4300 in shear and tensile tests. These tests revealed the tensile spring constant, Young modulus, shear modulus, tension, and shear capacity of each epoxy resin. It was concluded that ignoring progressive failure of epoxy resin and assuming the epoxy resin behaves in a linear brittle manner is conservative.

There are many studies about strain rates behavior of some carbon fiber composites materials and they are described as follow:

Material used	Strain rate (s^{-1}) range	Conclusions
Harding J. [5, 6]) Unidirectional-reinforced Carbon/epoxy plate. The Fiber were of type HYFIL-Torayca -130-s, with a resin system of type R7H and an epoxy similar to Araldite MY750	Dynamic test over 10^{-4} to 10^{3} considering impact rates of strain.	The tensile modulus, failure stress and failure mode were found to be strain rate insensitive.
Shim et al. [7]Carbon fiber filled liquid crystalline polymer (LCP) composites Vectra A230	Static loading 10^{-2} and Dynamic loading 400	The fracture strain and Young modulus were found to be influenced by changes in the strain rate.
Daniel et al. [8] Unidirectional laminates SP288/AS graphite/epoxy.	100 to 500	In fiber direction tensile modulus, shear modulus and shear strength are increased with strain rate whereas tensile strength, ultimate tensile strain and ultimate shear strain are insensitive to strain rate. In transversal direction modulus and strength are increased whereas ultimate strain is insensitive
Chamis CC. et al. [9] Resin 977-2 and IM7/977-2 carbon/epoxy composite. The 977-2 resin is an epoxy toughened with thermoplastic components.	$5x10^{-5}$ to 400	Young modulus is increased with increasing strain rate, the maximum stress is insensitive to strain rate increased and in general the composite sensitive to strain rate is driven by the resin behavior.

Most of the researches results confirm that Young modulus, shear modulus and shear strength are strain rate sensitive whereas, tensile stress, ultimate tensile stress and ultimate shear strain are strain rate insensitive. Besides, the strain rate sensitive composite behavior is driven by the resin behavior and the sort of load at which Carbon fiber composites materials are subjected.

Different researches have been made for carbon fiber composites materials but only some of them have focused on fractographic analysis before and after tests. M.D Gilchrist & N. Svensson[10] used SEM technique to study a fractographic features associated with delamination in multidirectional laminates of T300/914 carbon/epoxy composite, using DCB,ELS,FRMM and MMB fracture mechanics coupons, considering pure mode I, pure mode II and mixed modes I/II of loading under both static and fatigue conditions. From the results of the examination, a very large number of broken fiber seems to be a characteristic of mode I failure while; a larger amount of resin debris are present due to fatigue loading than in static failure; Therefore they characterized the different loadings modes using cusps angles and fiber pull-out on the fractures surfaces.

Most of the existing researches about adhesive bonding technology and composites materials are for those used in aeronautical and space science and other industries [11-14] but lack researches has been regarded to those polymers and composites material focus in civil engineering [15-17]. Nowadays does not exist any mandatory structural design code in any country around the world. There are guidelines or handbooks such as the Japanese (JSCE-1197), the American (ACI 440-2000) as well as the European (FIP-CEB-2001) but any of them have the same level of mandatory as ACI-318 for structural concrete design or AISC 360 for structural steel design in USA or the EURO codes in Europa. The reason why composite material and adhesive bonding materials do not have a mandatory design code in civil engineering is because; these materials have properties that change as long as their primary constituent change. In that sense, it is necessary to focus attention in the primary constituent behavior. Cohesive fracture is the desire failure mode when an adhesive bonding is used to fasten together two surfaces and a good adhesion between matrix and fibers (interphase) used as loading carrying component is also necessary in composite materials. Therefore, to study in a deeply way adhesive bonding and composite material mechanical behavior is an important contribution to this field. Nowadays, the majority of research in adhesive bonding and composites materials have been focused in determining mechanical properties, glass transition temperatures, lap shear behavior and other properties, using and/or developing different

methods. However, the majority of them have forgotten to study the morphology of cross section surface before and after failure occur, using Scanning Electron Microscopy (SEM) technique. The researches that have focused in cross section failured surfaces have considered polymers and composite materials used in another field different that civil engineering in order to enhance or change any behavior or mechanical property than the specific field as aeronautical or automotive industry requires. The main objectives of this research is to determine the strain rate dependent behavior of composites materials and epoxies, at low strain rates considering arbitrary loading rates; as well as studying adhesive bonding cross section failure surface and the interphase of matrix and fiber in composite materials using the Scanning Electron Microscopy (SEM) technique.

1.2 Thesis outline

This thesis is composed of eight sections, described as follow:

Section 1 introduces the actual lack of composite materials standards for civil engineering applications. Some researcher are mentioned focused on the sort of composites materials that are intended to study in this research. Moreover, it is introduced SEM technique, which is not a very common technique in civil engineering, but that some works using this technique are mentioned and the importance of it for civil engineering is highlighted. Section 2 presents the objectives of this research. Section 3 reviews some literature definitions about polymers and composite materials and civil engineering applications and strain rates definition. Section 4 presents in details materials and equipment used to develop this research. Section 5 presents uniaxial tests results under standard crosshead stroke rate and uniaxial tensile test under different strain rates. Discussion for each test and each material are also presented. Section 6 presents scanning electron microscopy results before and after tensile test for each material, failure surfaces are analyzed and compared. Section 7 presents the conclusions and recommendations reached in this research focused in civil engineering applications. Section 8 future works to reinforce and improve these results are presented.

2 OBJECTIVES

2.1 General objective

The present study is focused on determine the strain rate dependent behavior under low strain rate of carbon fiber reinforced polymer and its epoxy resin.

2.2 Specific objectives

1 To study composites materials using numerical methods to calculate its mechanicals properties.

2 To understand carbon fiber and epoxy resin mechanical behavior under tension test at low strain rates.

3 To analyze carbon fiber and epoxy material failure surface using scanning electron microscopy.

3 LITERATURE REVIEW

3.1 Polymers definition

Polymers are long 1D chains molecules of covalently bonded repeat units or 3D network of covalently bonded repeat units (monomers). The length of the molecule varies from 1,000 to 100,000 of atoms long. The following (Figure 1) is an epoxy monomer structures (Bisphenol A Diglycidyl Ether).

Figure 1- Epoxy monomer structure

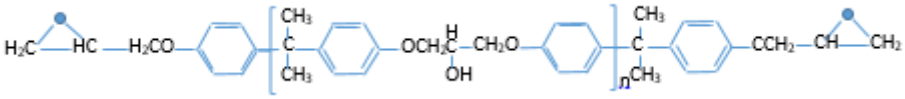

Source: Gotro (26).

The term polymer is commonly used today in the plastic and composites industry, and it is often used to imply the meaning of ¨plastic¨ or ¨resin¨. Actuality, the term polymer means much more.

Polymers can be both man made or from natural occurrence. For example, rubber is a natural polymer material that is extremely useful and has been used by mankind for thousands of years. Rubber has excellent elastic properties, and this is a result of the molecular polymer chain created by Mother Nature.

Both, man-made and natural polymers can exhibit elastic properties; however, polymers can exhibit a wide range of additional useful properties. Depending on the desired use, polymers can be finely tuned to leverage the advantageous property. These properties include reflective, impact resistant, tough, brittle, translucent, malleable, soft, elastic inelastic or insulated.

3.2 Main classes of polymers

Most polymers commonly referred to as plastic or thermoplastics are not cross-linked polymers, meaning the bonds between molecules and polymer chain can be broken and re-attached. Most common plastics can be bent into shapes with heat. They can also be recycled. Cross-linked polymers on the other hand cannot re-bond after the cross-linked bond between molecules is broken. Cross-linked polymers often exhibit desired properties such as higher strength, rigidity, thermal properties and hardness.

In fiber reinforced polymer (FRP) composite products, cross-linked polymers are most commonly used, and they are referred to as resin, or thermoset resin. The most common polymer used in composites are polyester, vinyl ester and epoxy.

Polymers that have covalent crosslinks can either be soft (like a rubber band) or hard (like cured epoxy). Crosslinks polymers are called thermosets because they cannot be re-processed into different shapes upon heating without permanent chemical degradation.

Linear and branched polymers (Figure 2) can be-reprocessed upon heating (or by dissolving them in a suitable solvent) and are termed thermoplastics.

Figure 2 - Alloy chains of polymers

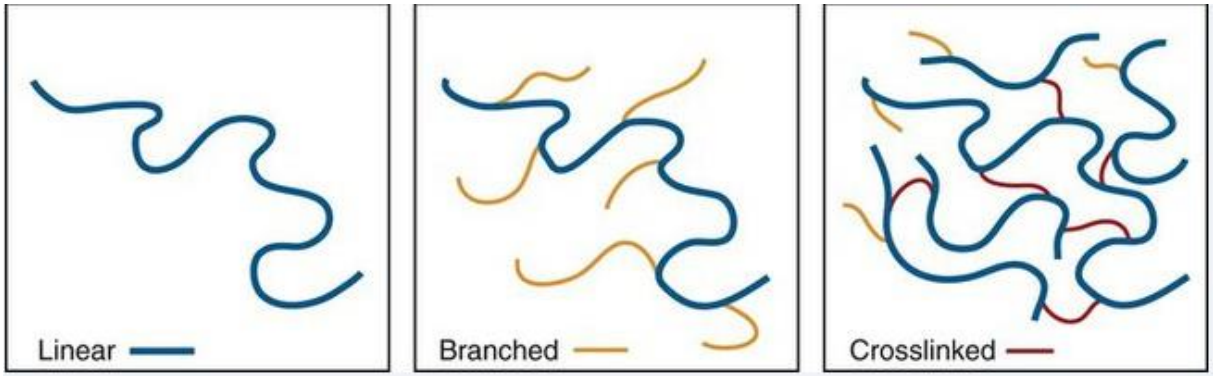

Source: Pocket dentistry (27).

Thermoplastics and thermosets polymers are sub-classified as follow: thermoplastic amorphous, thermoplastic semi crystalline, heat set elastomers and heat set thermosets.

Thermoplastic amorphous: polymers are 1-D covalently bonded chains. They are randomly oriented and form a glassy solid. When heated, they melt; when cooled, they solidify; and they can be remelted (melt recyclable).

Thermoplastic semi crystalline: Polymers also have 1-D covalently bonded chains. They form layers of thin; chain-folded crystalline lamellae separated by amorphous regions and are connected with tie molecules. When heated, they melt. When cooled, they solidify and can be re-melted (melt recyclable).

Heat set elastomers: are 3-D lightly to moderately crosslinked networks of long chain molecules that are covalently crosslinked during the curing. After the cure, the 3-D network maintains its structural integrity when heated (not melt recyclable).

Heat set thermosets: are 3-D high crosslinked network of covalently bonded molecules. The thermoset reaction forms a rigid amorphous solid with very good thermal resistance (not melt recyclable).

3.3 Polymer chains

A polymer is an organic material and the backbone of every organic material is a chain of carbon atoms. The carbon atom has four electrons in the outer shell. Each of these valence electrons can form a covalent bond to another carbon atom or to a foreign atom. The key to the polymer structure is that two carbon atoms can have up to three common bonds and still bonds with other atoms.

Thermoplastic materials can be pictured as a mass of intertwined worms randomly thrown into a pail. The binding forces are the result of Van der Waals forces between the molecules and the mechanical entanglement between the chains. When thermoplastic are heated, there is molecular movement and the bonds between molecules can be easily broken. This is why thermoplastic materials can be remolded.

Another group of polymers in which a single large network, instead of many molecules is formed during polymerization, since polymerization is initially accomplished by heating the raw materials and binning them together, is called thermosettings polymers. For this type of network structure to form, the mers must have more than two places for boning to occur; otherwise, only a linear structure is possible. These chains form jointed structures and rings, and may fold back and forth to take on partially crystalline structure.

Since these materials are essentially comprised of one giant molecule, there is not movement between molecules. Thermosetting polymers are more rigid and generally have higher strength than thermoplastic polymers. In addition, since there is no opportunity for motion between molecules in a thermosetting polymer, they will not become plastic when heated. Figure 3 and Figure 4 present the most common engineering thermoplastic and thermoset polymers.

Figure 3 - Common engineering Thermoplastics Polymers

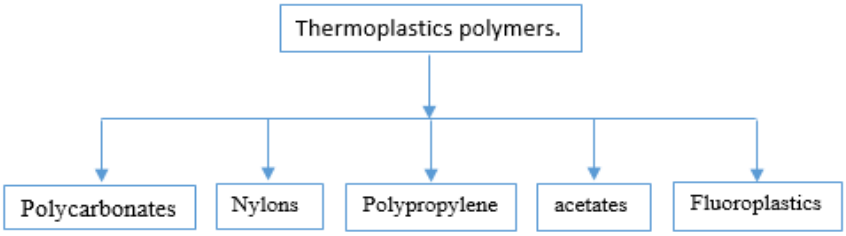

Source: by the author.

Figure 4 - Common engineering Thermosets Polymers

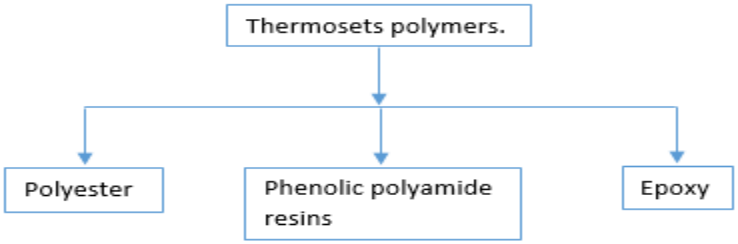

Source: by the author.

3.4 Polymer structure: crystallization, melting and glass transition

Long polymer chains can have a hard time crystallizing, since the individual chain gets tangled up and need to untangle to make a regular crystalline array. This is particularly true if the polymer melt is very viscous (which means its individual chains do not flow very easily) or if there are substituents on the chain that do not pack very well in the solid state.

Crystalline polymers usually contain regions of well-packed chains separated by amorphous regions. Pulling a fiber of linear polymer causes the chain to line up, and can induce crystallization. Snapping the plastic abruptly apart (before stretching it) is easier, because the chains do not have time to orient (Figure 5).

Figure 5 - Polymers crystalline array

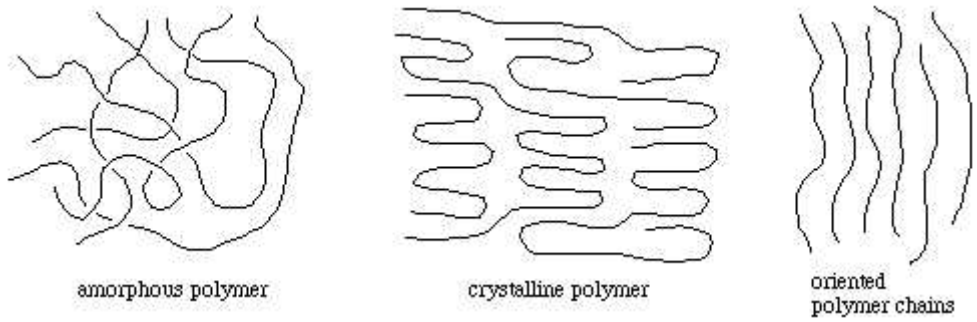

Source: Pennsylvania State University (28).

Besides viscosity, there are other factors influencing the ability of polymer to crystallize, one of them is the nature of the side groups on the polymer chains. With very bulky side groups or side groups that vary in an irregular way, the chains have a hard time organizing into an ordered, crystalline solid. This effect is important, because crystalline polymers tend to be much stiffer, harder and denser than amorphous polymers.

While small molecules always form crystals upon cooling, polymers, have another choice namely, glasses. Crystallization requires quite a bit of chain re-orientation (into a regular, ordered array) and if the chains are tangled enough or viscous enough, then they will not find the crystalline arrangement before solidifying. The result is a glassy solid in which the structure looks like the liquid, but the chains are no longer mobile.

In the glasses above melting point (Tm), the chains are fluid. At Tm they would like to be crystalline, since the crystalline form has lower molar volume (higher density), but cannot find the right orientation. At the glass transition temperature (Tg), the chains become frozen into a glass. Between Tm and Tg, the polymer is a metastable viscous liquid, in which the chain can undergo segmental motion. In the macroscopic sense, the polymer will be elastomeric above Tg and stiff below Tg.

There are several factors that influence the value of Tg, and determine the temperature range over which a polymer will be elastomeric or brittle. One of the most important is the flexibility of the polymer backbone, since chain motions generally require flexing of the backbone and rotation about intrachain bonds.

3.5 Composites materials

A composites material is made by combining two or more materials often that have very different properties. The two materials work together to give to the composites unique properties. However, within the composites you can easily tell the different apart as they do not dissolve or blend into each other. There are a lot natural composites found in animal and plants. Wood is a good example for plants, this is made from long cellulose fibers (a polymer) held together by a much weaker substance called lignin. The two weak substance –lignin and cellulose-together form a much stronger one. The bone in human body is also a composite, it is made from a hard brittle material called hydroxyapatite and a soft and flexible material called collagen. On its own, collagen would not be much used in the skeleton but it can combine with hydroxyapatite to give bone the properties that are needed to support the body.

People have been making composites for many thousands of years. One early example is mud bricks. Mud can be dried out into a brick shape to give a building material. It is strong for being squashed (it has good compressive strength) but it breaks quite easily when is bent (it has poor tensile strength). Straw seems easily for being stretched however easily for being crumpled up. By mixing mud and straw together, it is possible to make bricks that are resistant to both squeezing and tearing and make excellent building blocks.

The first modern composites material was fiberglass. It is still widely used nowadays for boat hulls, sport equipment, building panels and many car bodies. The matrix is a plastic and the reinforcement is glass that has been made into fine threads and often woven into a sort of cloth. On its own, the glass is very strong, but brittle, and it will break if bent sharply. The plastic matrix holds the glass fibers together and protects them from damage by sharing out the forces acting on them. Some advanced composites are now made using carbon fiber instead of glass. These materials are lighter and stronger than fiberglass but more expensive to produce. Carbon nanotubes have also been used successfully to make new composites. These are even lighter and stronger than composites made with ordinary carbon fiber but they are still extremely expensive. The biggest advantage of modern composites materials is that they are light as well as strong. By choosing an appropriate combination of matrix and reinforcement material, a new material can be made that exactly meets the requirements of a particular application.

3.5.1 Classification of composites

Composite materials are commonly classified at following two distinct levels:

The first level of classification is usually made with respect to the matrix constituent. The mayor composite classes include Organic Matrix composites (OMCs), Metal Matrix Composites (MMCs) and Ceramic Matrix Composites (CMCs). The term organic matrix composite is generally assumed to include two classes of composites, namely Polymer Matrix Composites (PMCs) and carbon matrix composites commonly referred to as carbon-carbon composites. Typical fibers include glass, aramid and carbon, which may be continuous or discontinuous. The continuous phase is the matrix, which is a polymer, metal, or ceramic. Polymer have low strength and stiffness, metal have intermediate strength and stiffness but high ductility, and ceramics have high strength and stiffness but are brittle. The matrix (continuous phase) performs several critical functions, including maintaining the fibers in the proper

orientation and spacing and protecting them from abrasion and the environments. In polymer and metal matrix composites that form a strong bond between the fiber and the matrix, the matrix transmits loads to the fibers through shear loading at the interface. In ceramic matrix composites, the objective is often to increase the toughness rather than the strength and stiffness, therefore a low interfacial strength bond is desirable.

The second level of classification refers to the reinforcement form-fiber reinforced composites, laminar composites and particulate composites. Fiber reinforced composites (FRC) can be further divided into those containing discontinuous or continuous fiber.

Fiber reinforced composites; are composed of fibers embedded in matrix material. Such a composite is considered a discontinuous fiber or short fiber composite if its properties vary with fiber length. On the other hand, when the length of the fiber is such that any further increase in length does not increase the elastic modulus of the composite, the composite is considered continuous fiber reinforced. Fiber are small in diameter and when pushed axially, they bend easily although they have very good tensile properties. These fibers must be supported to keep individual fibers from bending and buckling. A fiber has a length that is much greater than its diameter. The length-to- diameter (l/d) ratio is known as the aspect ratio and can vary greatly. Continuous fiber have long aspect ratios, while discontinuous fiber have short aspect ratios. Continuous fiber composites normally have a preferred orientation, while discontinuous fibers generally have a random orientation. Examples of continuous reinforcements include unidirectional, woven cloth and helical winding, while examples of discontinuous reinforcements are chopped fibers and random mat (Figure 6).

Figure 6 - Typical reinforcement types

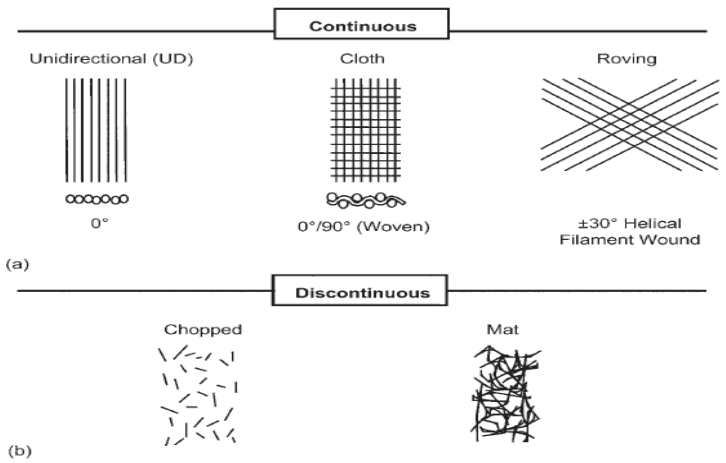

Source: Campbell (29).

Continuous fiber composites are often made into laminates by stacking single sheets of continuous fibers in different orientations to obtain the desired strength and stiffness properties with fiber volumes as high as 60 to 70 percent. Fibers produce high-strength composites because of their small diameter, they contain far fewer defects (normally surface defects) compared to the material produced in bulk. As general rule, the smaller the diameter of the fiber, the higher its strength, but often the cost increases as the diameter becomes smaller. In addition smaller-diameter high strength fiber have greater flexibility and are more amenable to fabrication process such as weaving or forming over radii.

These are composed of particles distributed or embedded in a matrix body. The particulate may be flakes or in powder form. Concrete and wood particleboards are examples of this category.

3.6 Composites materials and civil engineering

The European civil engineering community first considered FRP composite systems as a viable repair solution, research into the practical use of FRP systems was spearheaded in the 1960´s by the Swiss federal laboratories for materials testing and research (EMPA). The interest in FRP composite systems rise from the many drawbacks of post-strengthening structures with steel, the early work completed by the researchers' involved selecting fiber and adhesive types and findings feasible, safe employment of fiber systems. Researcher´s initially debated the benefits and drawbacks of various fiber material and mechanical properties, including fiber ratios and prestressing, in addition to finding cost/saving ratios for civil engineering projects.

These efforts concluded that carbon fiber reinforced polymers (CFRP) were the optimum fiber types and was a practical repair system for repairing beams, girder, towers, and columns. Previous research on FRP applications in engineering has increased understanding of the material for engineering applications. Retrofitting deficient structures with FRP laminates was initiated in Switzerland in the 1960´s (Meier, 1995). Since then several attempts have been made to advance the concept for wider applications in the remediation, strengthening and life-extension of civil engineering applications.

Fiber reinforced polymer (FRP) is a composite material that is composed of two components: fiber reinforcement and polymeric resin (matrix).The fiber enhance the strength and stiffness of the FRP composites while the matrix allows the load transfer between the individual fibers and protect them from mechanical and environmental damage. The properties

of the FRP composites depend on the properties of the matrix and the fiber as well as the fiber volume ratio and the fiber orientation.

CFRP composite is normally used in steel and concrete strengthening because its strength and stiffness are comparable to the steel material. There are three types of CFRP materials: normal modulus with stiffness lower than steel, high modulus (HM-CFRP) with a stiffness similar to steel and ultra-high modulus (UHM-CFRP) with stiffness higher than steel. The CFRP composites are supplied in forms of pultruded plates and as pre impregnated (prepreg) or dry wrap sheet and as rebar reinforcements. CFRP pultruded plates are bonded to the structure using a two parts epoxy adhesive, while CFRP sheet are bonded using an epoxy resin by wet lay-up technique.

Strengthening of existing structures is a necessity due to the destructive environmental conditions, increased service loads, as well as errors in design and during construction. Externally-bonded reinforcement (EBR) and near-surface mounted (NSM) reinforcement are the leading strengthening technique used for strengthening existing RC structures. The main drawback of EBR is that often suffers from premature debonding due to high shear stresses at the plate ends. In NSM strengthening the surrounding concrete protects the NSM bars or strips from thermal, environmental and mechanical damage. Improved durability stress-sharing mechanisms, and fatigue performance are other advantages due to the NSM reinforcement being placed inside the structural member.

Given the expanding FRP composite industry, new composite products have become commercially available for use and research in this field increased. CFRP grids have been researched as a reinforcing system of walls, FRP rods have been studied as reinforced of concrete slabs instead of conventional steel bars. Investigations have also been undertaken into the use of FRP rods as post-strengthening placed in epoxy filled holes of in-place walls and beams.

The plates are applied to the concrete surface using a similar adhesive to the one used for steel plate bonding. The initial grab of the adhesive is enough to hold the lightweight plate in place during the full cure period of the adhesive, eliminating the requirement for temporary works. The composite plates are 1.2-1.4mm thick. This means that any residual longitudinal forces in the end of the plate have a much smaller eccentricity to the concrete surface compared to steel plates. This means that peeling forces are lower which generally removes the requirement for anti-peel bolts.

Many steel beams has been retrofitted using carbon fiber plates and epoxies adhesive. Kim [18] found that when retrofitting using carbon fiber plate the stiffness of a damaged beam could reached up 86 % of the initial stiffness and increase 37% the load required to cause yield in an unrepair beam. However, the effect of the damage in the repaired beam is not mitigated, although the CFRP provides a noticeable strength gain, local plasticity at a damage location may still exist. Upon debonding of the CFRP, the stress is redistributed back into the steel tension flange and the CFRP stress is reduced. Täljsten [19] noticed that fatigue life of steel elements with non-pre-stressing CFRP retrofitting increases in average by a factor 2.86 and crack propagation decreases. Mertz [20] found that an undamaged beam increases 20% its stiffness by using a non-stressing bonded CFRP in the tension flange, moreover the yielding strength increases 42% .and when a damaged beam is retrofitted after lose 38% of its original stiffness, up to 83% of its original stiffness and 85% of its original flexural strength are restored. The premature failure mode is a failure of the adhesive bond, and is due to concentrations of shear and peeling stressing acting of the termination of the composite patch, and this mode is prevalent where shear forces are large relative to bending forces and large curvatures are present at the termination of the composite. Whereas for large girder where the span length causes small shear forces relative to bending forces and larger curvature are concentrated at midpoint this premature failure is avoided[20]. Therefore, it is found important to evaluate if strain rate sensitive behavior in the adhesive bond is causing premature failure by shear and peeling stressing concentrations.

To avoid premature failure mode of the adhesive bond Ghafoori[21] proposed a prestressing unbonded reinforcement (PUR) system that can be used when there is a concern about the effects of high ambient temperature, moisture, water and high cycle fatigue loading on the glue between the CFRP and the metal. The PUR system has a uniform stress distribution and a better fatigue performance than a prestressing bonded reinforcement system (PBR) and a different failure mode. As recommendation of the author the inflection point in the moment and shear diagrams must be considered when a CFRP retrofitting is proposed and a suitable CFRP length and anchorage must be properly detailed. As many research found retrofitting a steel beam using CFRP increase the beam stiffness and its fatigue life. Moreover, the originals mechanical properties of a damaged beam could be closely restore and enhance depending on the method used for retrofitting.

Amir [22] studied the behavior of concrete columns confined by fiber composites. It was observed that despite some volumes expansion beyond the critical stress of confined concrete, the linearly increasing hoop stress of FRP eventually curtails the volume expansion and reverse its direction. It is clear that with an adequate amount of external fiber composite, lateral expansion of concrete can be effectively curtailed. The confinement provided by transverse reinforcement or external jacket is of a passive type, in that confining pressure is developed only after the surrounded member undergoes hoop elongation (Poisson effect in concrete). The mechanics of confinement is therefore dependent on two factors, the tendency of concrete to dilate and the radial stiffness of the confining member to restrain the dilatation.

Dong [23] studied the structural behavior of RC beams externally strengthened with FRP sheets under fatigue and monotonic loading. It was observed that FRP strengthened beams have higher bending stiffness than non-strengthened beams. However, beams were not strengthened all over its longitudinal direction but its extremes nearby its supports as shear reinforcements. Moreover, post-fatigue monotonic tests showed that load deflection responses of the beams with and without previous fatigue loading are very similar until the final failure stage. In literature there are others studies which have been done in concrete and steel surfaces in order to understand much better the mechanical behavior of an element which have been retrofitted.

3.7 Strain rates

American metallurgist Jade Lecocq, who defined it as the rate at which strain occurs, first introduced the definition of strain rate in 1867. It is the time rate of change of strain. In Physics, the strain rate is generally defined as the derivative of the strain with respect to time. Its precise definition depends on how strain is measured.

Strain rate is the rate of change in strain of a material with respect to time. The strain rate at some point within the materials measures the rate at which the distances of adjacent parcels of the material change with time in the neighborhood of that point. It comprises both the rate at which the material is expanding or shrinking, and the rate at which it is being deformed by progressive shearing without changing its volume. It is zero if these distances do not change, as happens when all particles in some region are moving with the same velocity and or rotating with the same angular velocity, as if that part of the medium were a rigid body.

A single number can also express the strain rate when the material is being subjected to parallel shear without change of volume: namely, when the deformation can be described as a

set of infinitesimally thin parallel layers sliding against each other as if they were rigid sheets, in the same direction, without changing their spacing. This description fits the laminar flow of a fluid between two solids plates that slide parallel to each other or inside a circular pipe of constant cross-section. In those cases, the state of the material at some time can be described by the displacement of each layer, since an arbitrary starting time, as a function of its distance from the fixed wall. Then the strain in each layer can be expressed as the limit of the ratio between the current relative displacements of a nearby layer, divided by the spacing between the layers: therefore, the strain rate is where is the current linear speed of the material at distance from the wall.

The dynamic problem is complicated by such factors as the intensity of the loading, which influences the loading rate, wave propagation through the material and subsequently the type of damage occurring in the material and structure. To characterize and model materials/structures subjected to dynamic events, it is necessary to study the interactive nature of dynamic events occurring during the loading process. It is necessary in the design to delineate between material and structural response. Some considerations in this regards are:

Material response: Identified by insensitivity with respect to load application and specimen geometry (strain rate insensitive).

Structural response: Identified by sensitivity to both specimen geometry and material properties. Here the importance to study the strain rate dependent behavior of materials.

4 MATERIALS AND EQUIPMENT

In this work, the tensile behavior at different low strain rates of carbon fiber reinforced polymer (CFRP) was studied. Carbon fiber composite material Sikacarbodur S512 and polymer epoxies adhesives Sikadur 30 and Sikadur 330 were used. The equipment used for mechanical tests was a universal machine INSTRON/EMIC 23-200 from engineering department of UNESP-Bauru. Scanning electron microscopy (SEM) micrograph analysis were obtained using a field emission SEM (JEOL,model 7500F) equipment from the Institute of Chemistry in Araraquara.

The CFRP composites are supplied in the forms of pultruded plates and as preimpregnated (prepreg) or dry wrap sheets. CFRP pultruded plates are bonded to the structure using a two-part epoxy adhesive, while CFRP sheets are bonded using an epoxy resin by wet lay-up technique. Sikacarbodur S512 is a pultruded unidirectional carbon fiber plate of 1.2 mm thickness and 5 cm width, with carbon fibers longitudinal direction oriented parallel to plate longitudinal direction. It is done by pultrusion process in which dry, continuous fibers are pulled through a bath of resin and then through a mold. The mold serves two purposes: it forces the bundle of wet fiber to conform the desired shape and, since the mold is heated, it will cure the resin to set the bundle of fiber into its final shape. After the composite comes out of the mold, it is allowed to post-cure while being pulled to the saw where it will be cut to stock lengths. The raw resin is usually a thermosetting resin and it is sometimes combined with filler, catalysts and pigments. The fiber reinforcements becomes fully impregnated (wetted-out) with the resin such that all the fiber filaments are thoroughly saturated with the resin mixture. Sikacarbodur plate is bonded to the structure using a two-part epoxy adhesive in this case were considered Sikadur 30 and Sikadur 330.

Sikadur 30 is a solvent free epoxy adhesive, which is commonly used in bonding reinforcement of concrete and steel structures due to many advantages: first, it can be mixed and applied easily. Second, it can be cured at room temperature. Third, it has a high mechanical strength and high creep resistance. Fourth, it hardens without shrinkage and finally it is an excellent adhesion in damp conditions. This adhesive consists of two components: the epoxy resin (part A) and the hardener (part B) which are mixed together in a weight proportion of 3:1.

Sikadur 330 is a two part; solvent free, thixotropic epoxy based impregnating resin/adhesive. It is also a primer resin for the wet application system, impregnation resin for

the dry application method and structural adhesive for bonding CFRP plates to even surfaces. Its main advantages are described as follow: easy mix and application by trowel and impregnation roller, excellent application behavior to vertical and overhead surfaces, good adhesion to many substrates and high mechanical properties. This adhesive consists of two components: the epoxy resin (part A) and the hardener (part B) which are mixed together in a weight proportion of 4:1.

4.1 Standards tensile tests samples

Composite material uniaxial tensile tests were performed according to ASTM 3039/D3039M-14 Standard and epoxy material uniaxial tensile tests were performed according to ASTM D638 standard.

CFRP tensile tests were done using a load cell CCE100KN, for gripping the samples were used jaws GR012 with a maximum capacity of 100 kN and an electronic extensometer of 25 mm gage length was used. However, the extensometer did not fit very well maybe due to the small thickness of sample and it needed to be removed. Therefore, the tests were done without external extensometer. Polymer epoxies adhesive tensile tests were done using a load cell CCE2KN, for gripping the samples were used jaws GR003 with a maximum capacity of 2kN and an electronic extensometer of 25 mm of gage length was used.

In this study was first considered the standard tensile test for composite material at fiber direction, in this case Sikacarbodur S512, and then standards tensile test for epoxies adhesives. Then uniaxial tensile tests at different strain rate were conducted to obtain mechanical properties and to define the strain rate behavior of the considered materials. For standard uniaxial tensile test of Sikacarbodur S512 it was considered a standard head displacement rate of 2 mm/min and the specimen (Figure 7) follows the recommended dimension shown in table 2 of ASTM 3039/D3039M-14 standard. Standard tensile test of epoxy material (Figure 8) was done using a standard head displacement rate of 1 mm/min and specimen type IV (Figure 8) with a thickness of 5 mm.

Figure 7 - CFRP Standard tensile test sample

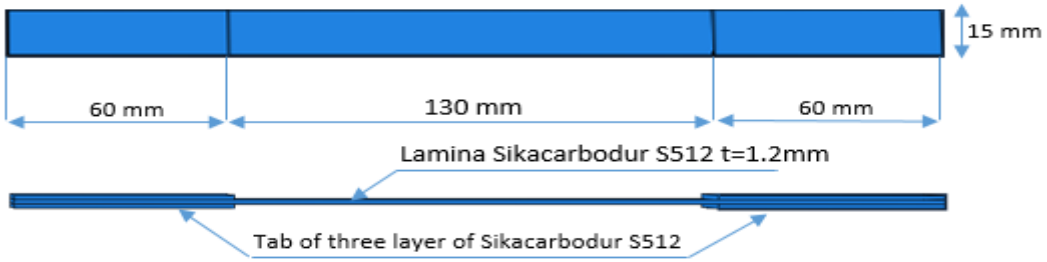

Source: Figures from 7 to 43 are own authorship.

Figure 8 - Epoxy resin tensile test sample

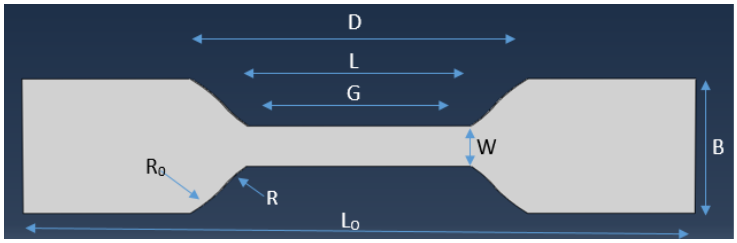

L_O=	115 mm
D =	65 mm
L =	33 mm
G =	25 mm
W =	6 mm
B =	19 mm
R_O=	25 mm
R =	14 mm

4.2 CFRP specimen for tensile test at different strain rates

Regarding Table 1 ¨tensile specimen geometry requirements¨ of ASTM D3039/D3039M-14 the specimen width and thickness must be selected to promote failure in the gage section. The same width and thickness of specimens used for standard tensile test were considered. Tensile test at crosshead stroke rate higher than the standard crosshead stroke rate promoted failure in the resin between the specimen and the tabs therefore, specimens without tabs were considered. However, the equipment was not able to hold the specimen due to its thickness; and; an emery cloth was used to wrap the specimen. After that, the specimen started to break in the middle of its width indicating that the equipment was gripping the specimen by its half width consequently, and a new specimen width was defined. In addition, a new minimum length was defined according to Table 1 of ASTM D3039/D3039M-14. The specimen dimension (Figure 9) for tensile test at different strain rates are shown below.

Figure 9 - CFRP tensile test specimen for different strain rate

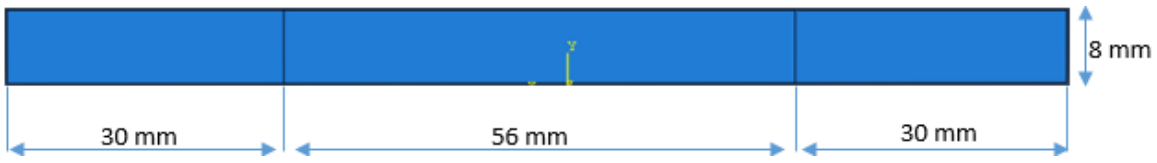

Because of the thickness of the specimen (1.2 mm) was not possible to use extensometer to measure the deformation. Therefore, the equipment used for the uniaxial tensile test measured the deformation. On the other hand, the gauge length was obtained subtracting a distance of 2 times the width of specimen from the distances between grips, then a gauge length of 40 mm was obtained and this gauge length is used to determine the nominal strain rate for every crosshead stroke rate used for tensile test.

For epoxy adhesive uniaxial tensile test at different strain rates, it was used samples with the same dimension than the ones used for standard tensile test. The dimension of the samples are shown in Figure 8.

4.3 Samples preparation

SIKA Company manufactures CFRP Sikacarbodur S512, Sikadur 30 and Sikadur 330 epoxies adhesives shown in Figure 10. CFRP Sikacarbodur S512 plate was cut using a metal cutting equipment (guillotine) with dimensions shown in Figure 7; the surface of sikacarbodur S512 was cleaned using acetone before sticking the tabs using Sikadur 30 adhesive, after this an emery cloth was use to assure a flat surface, tabs bevel angle of 90º was used. During the tension test was observed that many samples failed due to tab slippage, and those tests were discarded. A reason of that premature failure might be because after applying Sikadur 30 adhesive to stick the tabs to the main body of the sample was not applied any pressure, therefore the tabs were not properly stuck.

Figure 10 - Sika Company materials

In order to prepare the epoxy adhesive samples the first step was to prepare the molds; Using acrylic sheet and a laser equipment the molds of Sikadur 30 and Sikadur 330 samples were done, in the dimension presented in Figure 8. Considering that the material standard packaging is 6 Kg pre-dosed units (Component A + Component B) and that amount is higher than the required amount used in this work, the components were stirred using a mixing spindle

attached to a slow speed electric drill for about 3 minutes. Then each component was weighed using a balance AX200 (Shimadzu) and a plastic cup as shown in Figure 11 according to the required amounts following the proportion indicated in the each datasheets. The remaining material was stored properly in its original packaging in dry conditions at temperatures between 15^{o} C and 20^{o} C, protected from sunlight.

Figure 11 - Electronic scale model AX200

After weighting the components in the correct proportion, they were poured into a clean container first putting the component A and after the component B. Once they were together using a mixing spindle attached to a slow speed electric drill they were stirred for about 1 minute, until the material became smooth in consistency and in a uniform color then the molds were filled out with the material while it was within its potlife. However aeration while mixing was not avoided maybe due to the small amount of material stirred using the speed electric drill therefore, stirring the material with the two components together was done using a masonry spoon by hands as shown in Figure 12 then the molds were filled out as shown in Figure 13.

Figure 12 - Stirring procedure of component A and component B.

Figure 13 - Molds filled out with adhesive material.

After the molds were filled out, they were clamped and positioned on a mechanical press Figure 14, which will create pressure to them during the first 24 hours of curing.

Figure 14 - Pressure applied on adhesives material.

Once they were pressed during 24 hours, they were released as depicted in Figure 15 and positioned into an oven at 40º C temperature during six days to complete seven days of curing time.

Figure 15 - Samples in molds after applying pressure.

Once the samples cured, they were removed from the molds. To removing them, a hammer and a small sample of acrylic (obtained using the laser equipment to create the void where the adhesive was poured) were used. In the first attempt, the adhesive was strongly adhered to the acrylic molds and the samples were damaged while removing therefore, polidesmo 11 wax used in the molds before pouring the material to avoid the samples adhering to the molds and with a weak pushing the samples were released Figure 16.

Figure 16 - Samples removed from molds.

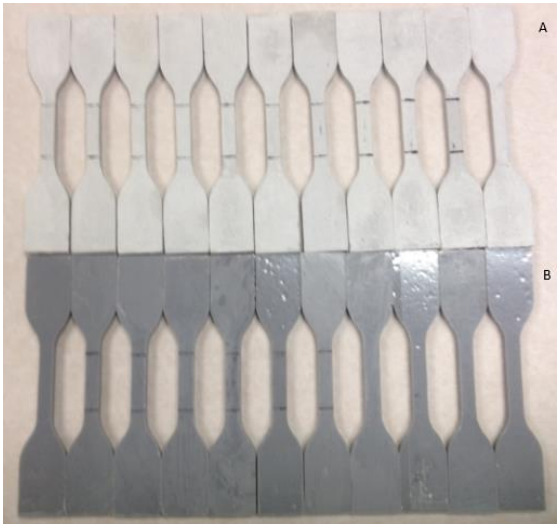

Figure 16 is showing just the samples that did not have any void or defect, to avoid any premature failure. After removing the samples, an emery cloth was used to uniform the thickness of the samples and to remove all the imperfection of the borders as marks of the molds or any other imperfection. This procedure was followed until the required amount of samples was reached. All the samples were kept into a clean and close container at room temperature for more than one month until the tensile tests were done.

For the microscopy analysis before and after tests, 3mmx3mm pieces of CFRP and 6mmx5mmx1mm pieces of adhesive samples were cut using an electric laboratory saw. Scanning electron microscopy (SEM) analysis were performed using a high resolution field emission SEM (JEOL, model 7500F). It was considered 5nm of carbon coating for epoxy resin; cases of epoxy resin images where carbon coating was not used are indicated nevertheless for CFRP micrograph were not considered any carbon coating. Special cares were regarded when cutting the samples after test to avoid any modification or contact that could distort the failed side of the samples. At least two samples of every material before and after tensile test were analyzed by microscopy.

5 UNIAXIAL TENSILE TESTS

5.1 Sikacarbodur S512 standard tensile test

The specimen was positioned on the testing machine, and the rate of test was settled at 2 mm/min. Some minutes after the test started, the specimen failed as shown in Figure 17 first with some delamination at zone A, then delamination at zone C, in opposite side of failure of zone A, and delamination process at zones A and C continues until zone B does not resist any load increment and it suddenly bursts. As the applied force is increasing, the specimen is being deformed and the resin, which bonds the carbon fibers, is being released and expelled, until the amount of bonded fibers remaining are not enough to resist the increment of force and suddenly bursts Figure 18. It is important to mention that some tests were discarded because they failed due to slippage in grips machine.

Figure 17 - CFRP Crack propagation.

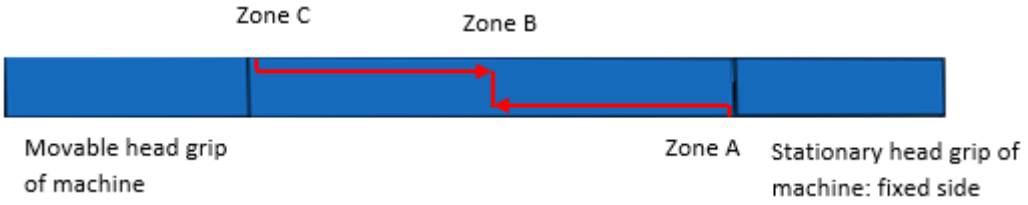

Figure 18 - CFRP Standard tension tests failed samples.

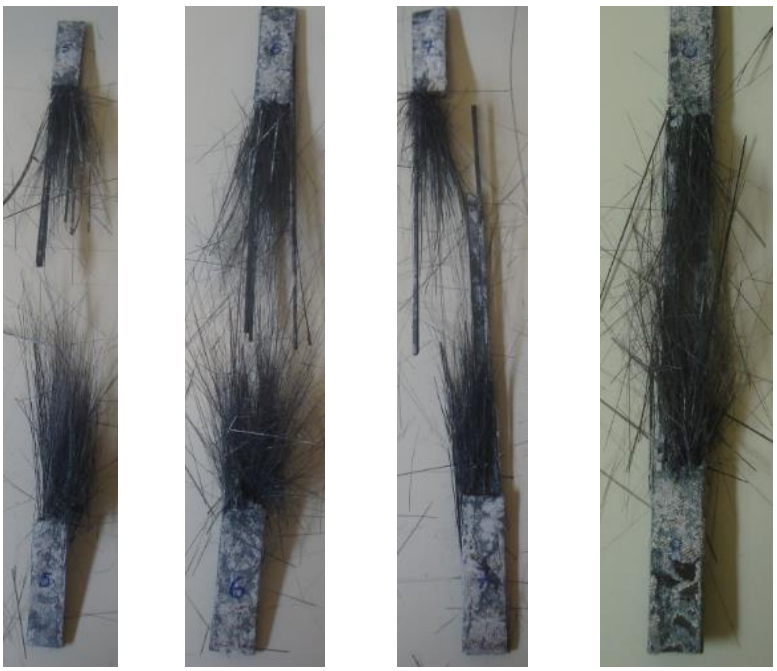

The stress-strain curves obtained from CFRP tension specimens are shown in Figure 19, presenting a linear relationship until failure. As observed all the specimens failed suddenly without sign of plastic deformation as shown in Figure 19. Therefore, Sikacarbodur S512 does not have plastic range, in terms of energy, the total dissipated energy is governed by the stored energy in elastic range, and Sikacarbodur S512 does not have recovery energy due to the lack of plastic range for ductile materials. However, high-energy dissipation capacity is a good indicator of performance.

The average yielding stress obtained at room temperature is 3,084 MPa, which is slightly higher than the value 2,800 MPa shown in datasheet of Sikacarbodur S512 and the average Young modulus is 163,152 MPa, which is also close to the value 165,000 MPa shown in datasheet of Sikacarbodur S512. These values prove that samples of excellent quality were prepared. The stress rates curves show that sikacarbodur S512 has a stress per unit of time of 12MPa/sec (635.52 MPa/min), a loading rate of 234 N/sec (12769.36 N/min) and a true strain rate of 7.3 x 10 -5 sec $^{-1}$(0.00438 min^{-1}) under static tensile test.

After analyzing Stress-strain curves of Sikacarbodur S512 obtained at room temperature with a standard head displacement rate of 2 mm/min (3.3E-02 mm/sec), it was found that Sikacarbodur S512 has not a ductile behavior and it is not able to sustain inelastic deformation since its energy dissipation is focused in elastic range.

The following graphs and tables show the results obtained for the samples for Sikacarbodur S512.

Figure 19 - CFRP Standard tensile tests stress-strain curves.

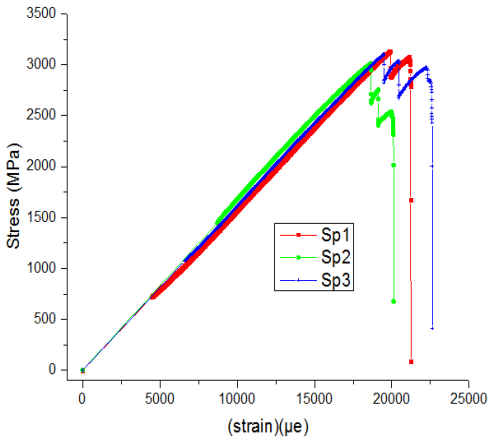

Note: 1000 (με) =0.001 (mm/mm) absolute strain.

Figure 20- CFRP standard tensile tests stressing and straining rates curves.

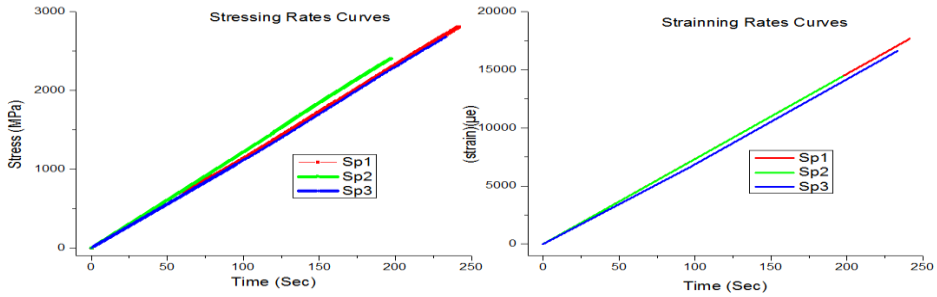

Table 1- CFRP tensile strength at standard tensile test.

Samples	Tensile strength (MPa)	Tensile strain to break (%)
Sp1	3137	1.99
Sp2	3014	1.86
Sp3	3100	1.95
Average	3084	1.93

Source: Tables from 1 to 17 are own authorship.

Table 2- CFRP Young modulus at standard tensile test.

Samples	Young modulus (MPa)	Stress rate (MPa/Sec)	Loading rate (N/Sec)	Strain rate (Sec-1)
Sp1	160878	12	233	7.3E-05
Sp2	166230	12	248	7.3E-05
Sp3	162347	11	221	7.3E-05
Average	163152	12	234	7.3E-05

5.2 Epoxy adhesive Sikadur 30 standard tensile test

Sikadur 30 tensile test was made first using 4 mm of samples thickness and 5mm/min, which is the speed of testing specified in ASTM D638 for specimen type IV. However, that speed made the samples failed in less than 0.5 minutes; Therefore, it was used a speed of testing of 1 mm/min and a specimen of 5 mm thick, to assure the samples fail close to 1 minute of testing. The nominal straining rate, regarding a gauge length of 25 mm is 0.04 min-1 (6.67 sec-1).Figure 21 shows samples after tensile test.

Figure 21- Photo of sikadur 30 Standard tensile test failed samples.

The Stress-Strain curves show a similar linear segment among samples at the beginning of the slope. However, tensile strength and strain to break are showing a little difference among them (Figure 22). The average Young modulus (Table 4) is 11,720 MPa, which is close to the value shown in datasheet (11,200 MPa). The average tensile strength (Table 3) is 30 MPa; this value is also close to the value reported in datasheet (31.0 MPa at 7 days curing time at 35 ºC).

The stressing rate curves (Figure 23) show an average stress rate (Table 4) of 0.37MPa/sec (22.20 MPa/min).The average loading rate is 11.68 N/sec (700.80N/min) and the average true straining rate is 3.0x10-5 sec-1 (0.00197 min-1). As expected, Sikadur 30 is a brittle resin as all thermoset resin, and has a tensile strength resistance of 1% of Sikacarbodur S512 tensile strength resistance, a Young modulus of 7 % of the Sikacarbodur S512 Young modulus and a smaller strain to break than a Sikacarbodur S512. Sikadur 30 stress-strain curves show that it does not have a considerable plastic range, but a non-linear elastic behavior is observed. Its elastic range governs the capacity to absorb energy. The yielding stress is not clearly defined due to the presence of a non-linear elastic behavior. In other words, the stress-strain curves do not show where the elastic range finish and where the plastic range starts. The following graphs and tables show the results obtained for the Sikadur 30 material.

Figure 22 - Sikadur 30 Standard tensile test stress-strain curves.

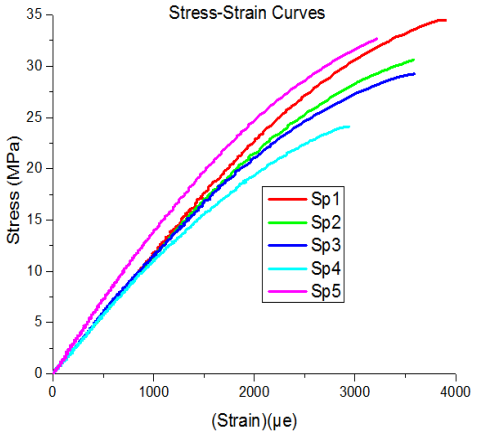

Note: 1000 (με) =0.001 absolute strain.

Figure 23 - Sikadur 30 Standard tensile test stressing and straining rates curves.

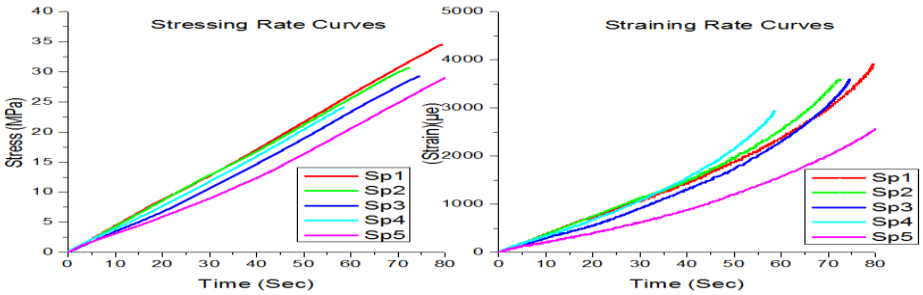

Table 3 - Sikadur 30 tensile strength at standard tensile test.

Samples	Tensile strength (MPa)	Tensile strain to break (%)
Sp1	35	0.39
Sp2	31	0.36
Sp3	29	0.36
Sp4	24	0.29
Sp5	29	0.32
average	30	0.34

Table 4 - Sikadur 30 Young modulus at standard tensile test.

Samples	Young modulus (MPa)	stress rate (MPa/Sec)	Loading rate (N/Sec)	Strain rate (Sec-1)
Sp1	11560	0.41	13.24	3.5E-05
Sp2	11460	0.43	12.92	3.5E-05
Sp3	11934	0.35	11.86	2.9E-05
Sp4	11315	0.37	11.22	3.3E-05
Sp5	12330	0.27	9.15	2.2E-05
Average	11720	0.37	11.68	3.0E-05

5.3 Epoxy adhesive Sikadur 330 standard tensile test

Sikadur 330 standard tensile test was conducted using the same sample dimension shown in Figure 8 and at the same condition of tensile test considered for Sikadur 30. Figure 24 shows samples after tensile test, as can be observed samples failed in the gauge length.

Figure 24 - Photo of Sikadur 330 tensile test samples.

Figure 25 presents the stress-strain curves of sikadur 330 and a nonlinear elastic behavior of the material is observed. Some samples failed before reach its tensile strength due to bubble of air inside the necking region and they were discarded. The average tensile strength obtained (Table 5) was 28 MPa and the average Young modulus (Table 6) was 3733 MPa. Both values are lower than the values shown in datasheet, which are 30 MPa and 4500 MPa respectively. The obtained average strain to break (Table 5) was 0.86%, which is similar to the reported strain to break shown in the material datasheet. Although the obtained values were lower than the values reported in datasheet, they were considered accurate because they were obtained at similar condition that could be found in any other project, i.e., without any special processing. The stressing rate curves (Figure 25) show an average stress rate (Table 6) of 0.25 MPa/sec (15 MPa/min). The average loading rate is 7.87 N/sec (472 N/min) and the average true straining rate is 6.68×10^{-5} sec (0.00197 min^{-1}).

The stress-strain curves show that sikadur330 has a predominated nonlinear elastic behavior, which defines its capacity to absorb energy but the yielding stress is not clearly defined. When comparing stress-strain behavior of sikadur 30 and sikadur 330 it is noticed that,

sikadur 330 has better seismic behavior than sikadur 30 since both have almost the same tensile strength but sikadur 330 has the biggest strain to break, more than twice. Moreover, Sikadur 330 has better energy dissipation capacity as can be observed in Figure 25 b. However, both resins present similar values in material datasheets and differences in tensile properties are not as remarkable as the results found in this study, which shows similar results of sikadur 30 with those presented by Hassein[2] when strain to break is considered. Therefore, a deeply study is recommended to assure the tensile strain to break behavior of materials. Both resins present two region, the first one is characterized by an elastic behavior and the second one is characterized by a nonlinear viscous-elastic behavior. A deeply study of these regions will define the yielding point of both resin and these values are not defined in datasheet values.

Figure 25 - Sikadur 330 standard tensile test stress-strain curves.

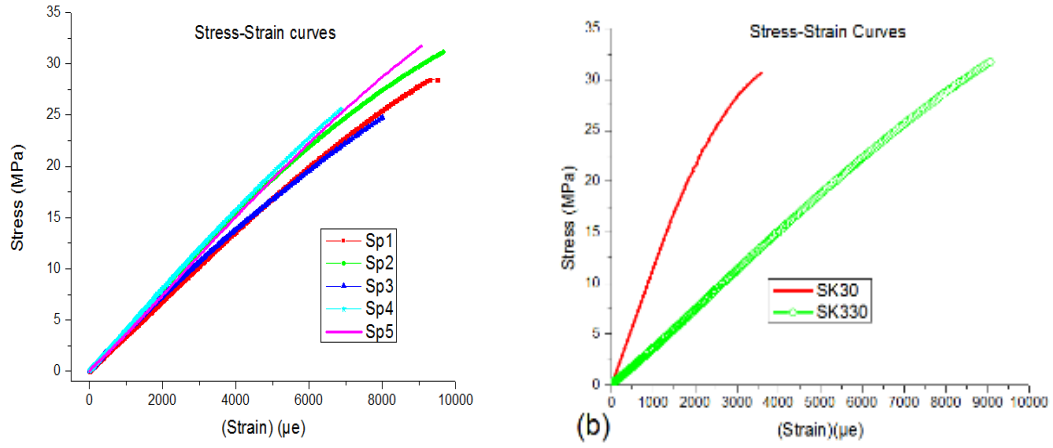

Note: 1000 (με) =0.001 absolute strain.

Figure 26 - Sikadur 330 standard tensile test stressing and straining rates curves.

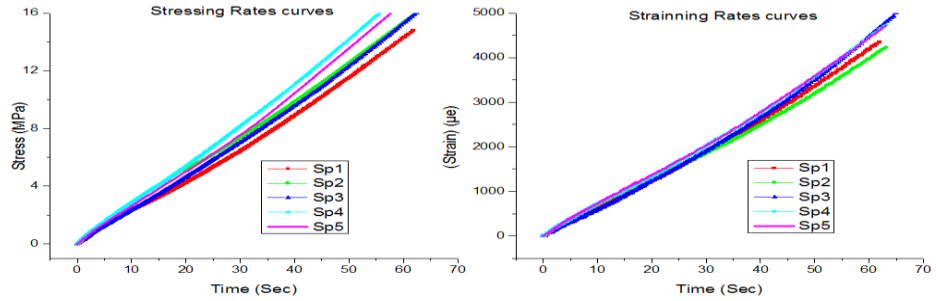

Table 5 - Sikadur 330 tensile strength at standard tensile test.

Samples	Tensile strength (MPa)	Tensile strain to break (%)
Sp1	28	0.93
Sp2	31	0.97
Sp3	25	0.80
Sp4	26	0.69
Sp5	32	0.91
average	28	0.86

Table 6 - Sikadur 330 Young modulus at standard tensile test.

Samples	Young modulus (MPa)	stress rate (MPa/Sec)	Loading rate (N/Sec)	Strain rate (Sec-1)
Sp1	3403	0.23	7.53	6.67E-05
Sp2	3889	0.26	8.14	6.44E-05
Sp3	3618	0.23	7.59	6.44E-05
Sp4	3984	0.27	8.23	6.89E-05
Sp5	3772	0.26	7.88	6.97E-05
average	3733	0.25	7.87	6.68E-05

5.4 Tensile test at different strain rates

5.4.1 Composite material Sikacarbodur S512

Tensile tests were conducted at three crosshead stroke rates: 0.5 mm/sec, 1 mm/sec and 2 mm/sec. The results are compared with tensile test conducted at standard crosshead stroke rate 0.03 mm/sec (hereafter known as standard tensile test). The nominal strain rate are calculated by dividing the stroke rate of the cross-head of the machine by the gauge length of the specimen, the nominal strain rates are 0.01 s-1, 0.03 s-1 and 0.05 s-1. The true strain rates are obtained directly from the data after the tensile test and these ones are selected to determine the strain rate behavior. To compare results between standard tensile tests and tensile test at different cross-head stroke rates, standard tensile tests were conducted regarding the specimen with the same dimension that shown in Figure 7. Then those results were compared with the obtained results using the specimen (Figure 9) defined following the recommendation found in the standard for unidirectional composites material table 2 ¨tensile specimen geometry recommendations¨. The results are shown in the table below.

Table 7- CFRP standard tensile test results under different specimens sizes.

Samples	Young modulus (MPa)		Tensile strength (MPa)		Tensile strain to break (%)	
	specimen1	specimen2	specimen1	specimen2	specimen1	specimen2
Sp-1	160878	161800	3137	3154	1.99	2.01
Sp-2	166230	163982	3014	2867	1.86	1.93
Sp-3	162347	165670	3100	3067	1.95	2.17
Average	163152	163817	3084	3029	1.93	2.04

In Table 7 specimen1 is referred to the specimen shown in Figure 7 and specimen2 is referred to the specimen shown in Figure 9. Both specimens were subjected to at cross-head stroke rate of 2 mm/min (0.03 mm/sec) as recommended for the standard. As both kind of specimens presented similar results, the results from specimen1 will be used to analyze the strain rate behavior of this composite material. Hereafter when in this document is mentioned standard tensile test means the results obtained with specimen1 at a cross-head stroke rate of 2mm/min (0.03 mm/sec). In addition, when mentioned standard strain rate means true strain rate when standard tensile is considered.

Table 8 to Table 10 show the obtained results for CFRP uniaxial tensile test. When compare the standard tensile test results with the results obtained at different strain rate, it is observed that the Young modulus and strain to break are influenced by strain rate behavior whereas tensile strength and the absorbed energy the strain rate effects could be neglected.

Table 8 - CFRP Young modulus and tensile strength at different strain rates.

Nominal Strain rate (s-1)	Young modulus (MPa)				Tensile strength (MPa)			
	Specimen1	1.E-02	3.E-02	5.E-02	Specimen1	1.E-02	3.E-02	5.E-02
Sp-1	160878	141203	141096	144937	3137	2975	3053	3268
Sp-2	166230	150152	146874	145696	3014	3111	3134	3008
Sp-3	162347	152196	145144	144376	3100	3059	3515	3273
Average	163152	147850	144371	145003	3084	3048	3234	3183
Std deviation (%)	1.4	3.2	1.7	0.37	1.67	1.84	6.23	3.89

Table 9 - CFRP tensile strain to break and absorbed energy at different strain rates.

Nominal strain rate (s-1)	Tensile strain to break (%)				Absorbed energy (MJ/m3)			
	Specimen1	1.E-02	3.E-02	5.E-02	Specimen1	1.E-02	3.E-02	5.E-02
Sp-1	1.99	2.1	2.19	2.29	35.28	32.57	34.05	39.09
Sp-2	1.86	2.15	2.41	2.23	32.64	35.33	41.42	38.92
Sp-3	1.95	2.02	2.42	2.30	39.65	31.43	42.69	39.89
Average	1.93	2.09	2.34	2.27	35.86	33.11	39.39	39.30
Std deviation (%)	2.82	2.56	4.54	1.37	8.06	4.95	9.67	1.08

Table 10 - CFRP strain rate behavior.

True strain rate (s^{-1})	Young modulus (MPa)	Tensile strength (MPa)	Strain to break (%)	Absorbed energy (MJ/m^3)
7.30E-05	163152	3084	1.93	35.86
2.02E-03	147850	3048	2.09	33.11
4.03E-03	144371	3234	2.34	39.39
8.06E-03	145003	3183	2.27	39.30

Figure 27 shows time vs strain rates of CFRP. It is observed that the time of failure of every sample is inversely proportional to the strain rate used, this means the shortest time of failure for the highest strain rate. It is also observed that although the strain to break increases when increasing strain rate, the tensile strength remains unchanged and the time of failure decreases up to 3 seconds. This indicates that the same load applied in a faster way will provoke a bigger deformation in a shorter time.

Figure 28a Shows the Young modulus vs strain rates of CFRP. The Young modulus obtained at standard tensile test is the reference line and it shows the variation of the Young modulus correlated to different strain rates. It is observed that Young modulus decreases approximately 12 % when strain rate increases defining the strain rate dependent behavior of the material. However, regarding the loading conditions at which the retrofitting element will be subjected to, this decrease in the Young modulus must be considered or neglected.

Figure 28b shows the tensile strength vs strain rates of CFRP. The tensile strength obtained at standard tensile test is the reference line and it shows the variation of the tensile strength correlated to different strain rates. Considering standard deviation, it is observed that the tensile strength is strain rate insensitive. Therefore, obtained results at standard tensile test may be used for structural design.

Figure 28c shows the strain to break vs strain rates of CFRP. The strain to break obtained at standard tensile test is the reference line and it shows the variation of the strain to break correlated to different strain rates. It is observed that the strain to break increases approximately 15% when strain rate increases from standard strain rate but regarding differences among strain rates, neglecting the standard strain rate, that increment is 7% respect to the lowest strain rate, this is indicating that from standard strain rate until the lowest strain rate the increment is 8%. Therefore, the strain to break is showing a strain rate dependence. For structural design, the strain to break increment must be neglected because the main increment occurs at the highest strain rates (the shortest time of failure) considered in this research.

Figure *28*d shows the absorbed energy vs strain rates of CFRP. The absorbed energy obtained at standard tensile test is the reference line and it shows the variation of the absorbed energy correlated to different strain rates. It is observed that according with standard deviation the absorbed energy is strain rate insensitive. The absorbed energy is the area under the stress-strain curves therefore the Young modulus, strain to break and tensile strength influence on it. When strain rates are considered for Sikacarbodur S512 the tensile strength remaines constant, the Young modulus decreases but the strain to break increases and the absorbed energy does not change (Figure 28). It is important to highlight that all the absorbed energy is in the elastic range and it has the same behavior under different strain rates. A remarkable difference in failure mechanism is not observed due to the increments in strain rates for uniaxial tensile tests.

It is important to know the strain rate behavior of this composite material because it may be a factor to consider when an element needs to be retrofitted. Regarding the results presented in this documents Sikacarbodurs512 has a brittle failure and its failure mechanism does not change due to different strain rates. This is important because it has a very well defined behavior, which means that the level of confidence in structural retrofitting design of this material is as high as the level of confidence of steel or concrete materials. Because the absorbed energy remains constant when tested at different strain rates, this material could be used to retrofit any element when it is required. However, special care must be considered to ensure than the level of performance of the retrofitted element will be developed just in its elastic range. Once the Sikacarbodur failed all the stresses are transferred back to the main element[(18)].

Figure 27- CFRP strain rate behavior.

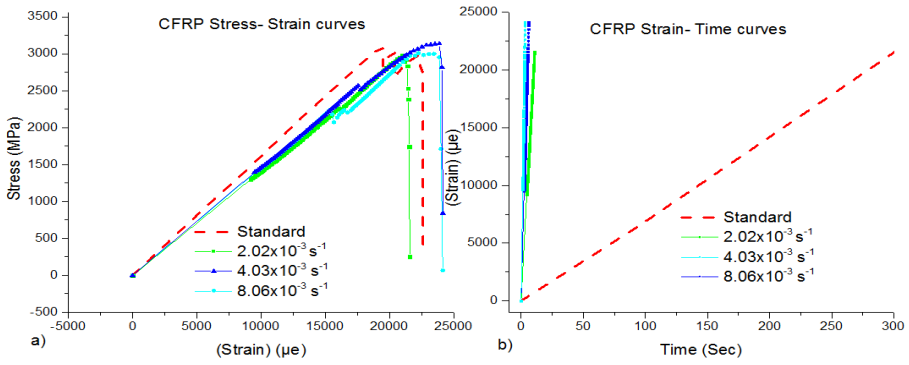

Figure a: Stress-Strain curves relationship. Figure b: Strain-Time curves relationship.

Note: 1000 (με) =0.001 absolute strain.

Figure 28- CFRP strain rate behavior vs standard tensile test behavior.

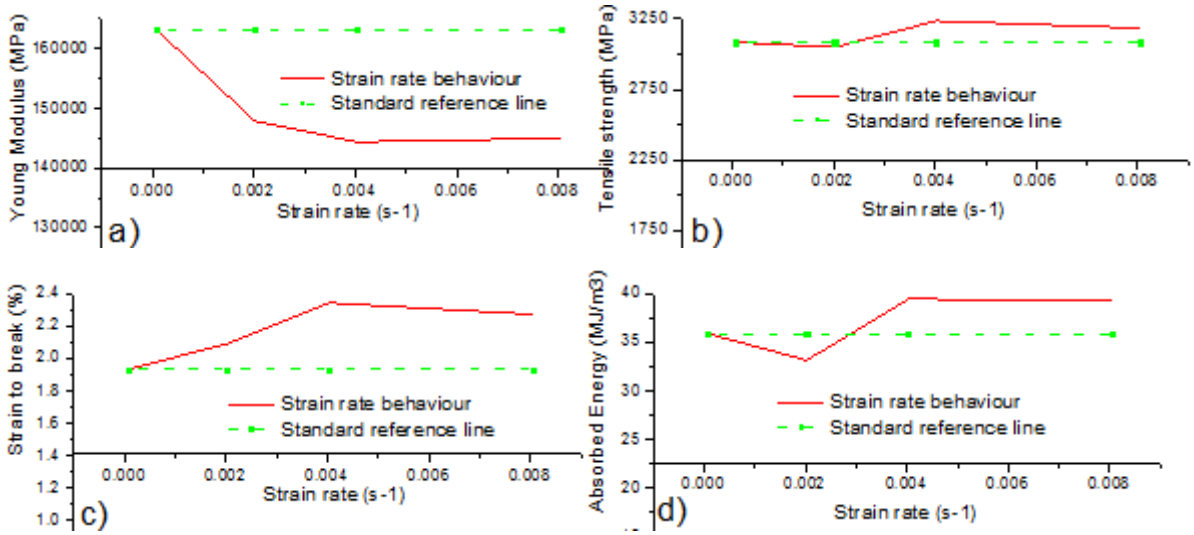

Figure a: Young modulus vs Strain rates curve. Figure b: Tensile strength vs Strain rates curve. Figure c: Strain to break vs Strain rates curve. Figure d: Absorbed energy vs Strain rates curve.

5.4.2 Sikadur30 tensile test at different strain rates

Considering a gauge length of 25 mm (Figure 8) and tensile test at three crosshead stroke rates of 0.5 mm/sec, 1 mm/sec and 2 mm/sec, the nominal strain rates are 0.02 s-1, 0.04 s-1 and 0.08 s-1. On the other hand, the true strain rates are obtained directly from the data after tensile test. The tensile test results under standard crosshead stroke rate (hereafter known as standard tensile test) will be used as a benchmark against true strain rates results to determine the strain rate behavior of the material.

Table 11 to Table 13 show the results obtained at different strain rates compared with the standard tensile test results. The results obtained considering a nominal strain rate 0.08 s-1 were discarded. It was found some inconsistences in the measured data, maybe because of the high crosshead stroke rate of the machine, the extensometer slipped in almost all the specimens and was not possible to obtain a minimum number of accepted tests. The results show that the Young modulus is influenced by strain rates, whereas the tensile strength, the tensile strain to break and the absorbed energy are not influenced by strain rates. Table 13 shows the true strain rates at which the specimens are subjected and it shows the average of the mechanical properties studied in this paper.

Table 11- Sikadur 30 Young modulus and tensile strength at different strain rates.

Nominal strain rate (S-1)	Young modulus (MPa)			Tensile strength (MPa)		
	Standard test	2.E-02	4.E-02	Standard test	2.E-02	4.E-02
SP-1	11560	10936	10332	35	29	28
Sp-2	11460	10786	10439	31	35	38
Sp-3	11934	11789	10559	29	35	25
Sp-4	11315	10863	10504	24	26	40
Sp-5	12330	11324	10068	29	32	39
Average	11720	11140	10380	30	31	34
Std deviation (%)	3.13	3.36	1.67	11.93	11.36	18.32

Table 12- Sikadur 30 tensile strain to break and absorbed energy at different strain rates.

Nominal strain rate (S-1)	Tensile strain to break (%)			Absorbed energy (MJ/m3)		
	Standard test	2.E-02	4.E-02	Standard test	2.E-02	4.E-02
SP-1	0.39	0.28	0.32	0.08	0.04	0.05
Sp-2	0.36	0.37	0.49	0.06	0.07	0.11
Sp-3	0.36	0.37	0.26	0.06	0.08	0.04
Sp-4	0.29	0.29	0.45	0.04	0.04	0.1
Sp-5	0.32	0.34	0.45	0.08	0.06	0.1
Average	0.34	0.33	0.39	0.06	0.06	0.08
Std deviation (%)	10.37	11.66	22.65	25.82	26.87	36.23

Table 13- Sikadur 30 strain rates behavior.

True strain rate (S^{-1})	Young modulus (MPa)	Tensile strength (MPa)	Strain to break (%)	Absorbed energy (MJ/m^3)
3E-05	11720	30	0.30	0.06
7E-04	11140	31	0.3	0.06
2E-03	10380	34	0.4	0.08

Figure 29a shows the stress-strain curves of sikadur30 obtained at different strain rates compared with the stress- strain curve obtained at standard tensile test. The plot shows that in the beginning of the curve (linear behavior) the standard tensile test has the biggest slope whereas the curves at different strain rates show the biggest tensile strength and strain to break.

Figure 29b shows strain vs time curves of sikadur 30 at different strain rates compared with the strain vs time curve at standard tensile test. The plot shows that the strain to break at 7x10 -4 s-1 strain rate (0.5 mm/sec crosshead stroke rate) remains almost constant correlated with the strain to break at standard tensile test, but the time of failure decreases up to 3.5

seconds. When a strain rate of 2x10-3 s-1 is applied the strain to break increases and time of failure decreases up to 1.7 seconds. The plot is indicating the damage in the material increases in a short time when it is subjected to a suddenly external load.

Figure 30a shows the Young modulus vs strain rates for Sikadur 30. The curve shows that the Young modulus decreases when increasing the strain rates. The Young modulus decreases approximatively 10 % correlated to standard tensile test. Regarding the loading conditions at which the retrofitting element will be subjected to, this decrease in Young modulus must be considered or neglected.

Figure 30b shows the tensile strength vs strain rates for Sikadur 30, the curve shows that the tensile strength has a small increment when increasing the strain rate. The tensile strength increases approximated 8% correlated to standard tensile test however that increment is smaller than standard deviations therefore, the tensile strength is strain rate insensitive

Figure 30c shows the strain to break vs strain rates for Sikadur 30. The curve shows that the strain to break is strain rate insensitive because it shows a not remarkable strain to break increment when strain rates are increased.

Figure 30d shows the absorbed energy vs strain rates for Sikadur 30. The curve shows that the absorbed energy is strain rate insensitive. The absorbed energy increases approximated 15 % correlated to standard tensile test and that increment is already taken when standard deviation is considered.

Regarding Figure 29a, it is observed that the elastic range of the material is increased when increasing strain rates; however, that elastic range is not necessary defined by a linear behavior, a nonlinear elastic behavior is observed and that behavior must be studied deeply to define the yielding stress of the material. It was not observed diffuse in cross section when strain rate was increased therefore all the specimens shown a brittle behavior.

Figure 29 - Sikadur 30 strain rate behavior.

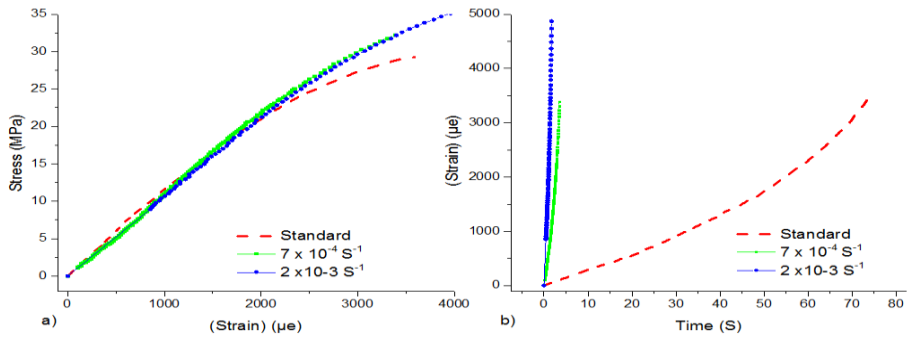

Figure a: Stress-Strain curves relationship. Figure b: Strain-Time curves relationship.

Note: 1000 (με) =0.001 absolute strain.

Figure 30 - Sikadur30 strain rate behavior vs standard tensile test behavior.

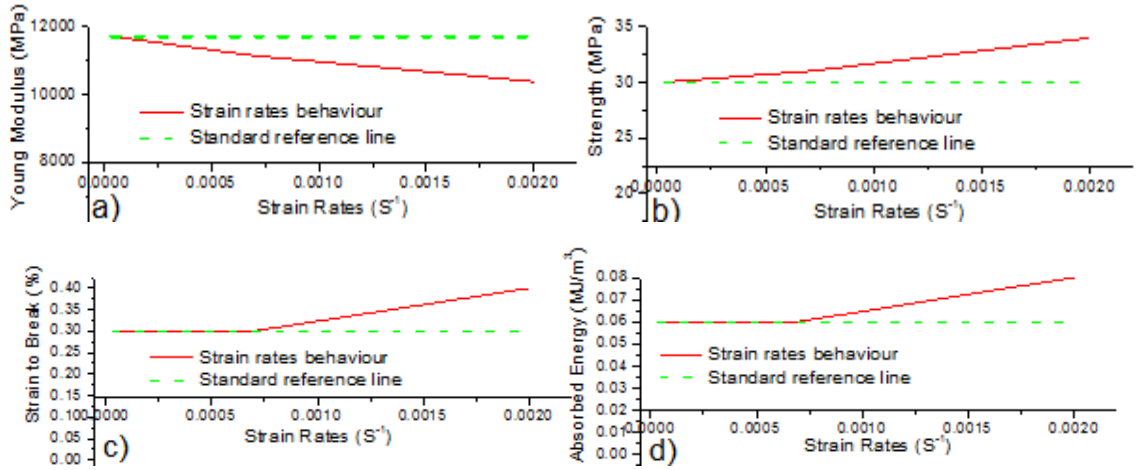

Figure a: Young modulus vs Strain rates curve. Figure b. Tensile strength vs Strain rates curve. Figure c: Strain to break vs Strain rates curve. Figure d: Absorbed energy vs Strain rates curve.

5.4.3 Sikadur 330 tensile test at different strain rates

Sikadur 330 tensile test at different strain rates were performed under the same conditions indicated for sikadur 30 in section 5.4.2.

Table 14 to Table 16 show the results obtained at different strain rates compared with the standard tensile test results. As observed for sikadur 30 the results obtained considering a nominal strain rate 0.08 s-1 were discarded, because it was not possible to obtain a minimum number of accepted tests. The results show that the Young modulus is strain rate insensitive whereas, the tensile strength, tensile strain to break and the absorbed energy are influenced by

strain rates. Table 16 shows the true strain rates at which the specimens are subjected and it shows the average of the mechanical properties studied in this paper.

Table 14 - Sikadur 330 Young modulus and tensile strength at different strain rates.

Nominal strain rate (S-1)	Young modulus (MPa)			Tensile strength (MPa)		
	Standard test	2.E-02	4.E-02	Standard test	2.E-02	4.E-02
SP-1	3403	3787	3700	28	34	41
Sp-2	3889	3708	3505	31	43	43
Sp-3	3618	3797	4348	25	42	46
Sp-4	3984	3640	3747	26	41	41
Sp-5	3772	3760	3932	32	35	45
Average	3733	3738	3846	28	39	43
Std deviation (%)	5.5	1.55	7.42	9.85	9.59	4.77

Table 15 - Sikadur 330 tensile strain to break and absorbed energy at different strain rates.

Nominal strain rate (S-1)	Tensile strain to break (%)			Absorbed energy (MJ/m3)		
	Standard test	2.E-02	4.E-02	Standard test	2.E-02	4.E-02
SP-1	0.93	0.95	1.26	0.14	0.17	0.28
Sp-2	0.97	1.25	1.36	0.17	0.28	0.31
Sp-3	0.80	1.26	1.24	0.11	0.28	0.32
Sp-4	0.69	1.27	1.17	0.1	0.28	0.25
Sp-5	0.91	0.96	1.29	0.15	0.17	0.31
Average	0.86	1.14	1.26	0.13	0.24	0.29
Std deviation (%)	11.86	13.12	4.94	20.06	22.52	9.00

Table 16 - Sikadur 330 strain rate behavior.

True strain rate (S^{-1})	Young modulus (MPa)	Tensile strength (MPa)	Strain to break (%)	Absorbed energy (MJ/m^3)
7E-05	3733	28	0.86	0.13
2E-03	3738	39	1.14	0.24
4E-03	3846	43	1.26	0.29

Figure 31a. shows the stress-strain curves for Sikadur 330 at different strain rates compared with stress-strain curves at standard tensile test. It is observed that the tensile strength, strain to break and absorbed energy increase when increasing the strain rate correlated to standard tensile test. However regarding strain rates different than the standard strain rate the differences between mechanical properties are reduced this means that when increasing the strain rate correlated to another strain rate different from the standard strain rate the damage suffered by the material is the same.

Figure 31b shows the strain- time curves for Sikadur 330 at different strain rates compared with standard tensile test curve. It is observed that the strain to break increases when increasing strain rates although time of failure keeps short (2.5 seconds at the highest strain rate). The plot is indicating that the damage in the material increases in a short time when it is subjected to a suddenly external load.

Figure 32a shows Young modulus-strain rates curve for Sikadur 330.The reference line represents the value of the standard tensile test result and it is used to determinate the Young modulus behavior at different strain rates. Young modulus increases 2 % when increasing the strain rate. That increment is smaller than standard deviations therefore the young modulus is strain rate insensitive and for structural design Young modulus at standard tensile test must be used.

Figure 32b shows the tensile strength-strain rates curves for sikadur 330. The standard reference lines represent the tensile strength obtained at standard strain rate. The tensile strength increases when increasing the strain rates, an increment of 45 % is obtained correlated to standard tensile test result. However when compared strength between strain rates the increment is 10%, this indicates than the tensile strength is rate dependent and the biggest increments occur at lowest strain rates and it remains with small increments when strain rates are incremented. For structural design to consider tensile strength obtained at standard tensile test is recommended due to the small difference in time of failure (Figure 31b) between strain rates.

Figure 32c shows the strain to break-strain rates curves for Sikadur 330. The plot shows an increment of 40% of strain to break correlated to standard tensile test result. However, the increment is 10% when considering just strain rates different from standard strain rate. This is indicating that strain to break is strain rate dependent and the biggest increment occurs at lowest strain rates therefore the standard tensile test results must be considering for structural designs.

Figure 32d shows the absorbed energy- strain rates curve. The plot shows that the absorbed energy increases when increasing the strain rates correlated to standard strain rate, an increment of 100% is obtained. However, when standard strain rate is not considered the increment of absorbed energy is 20%, indicating than the biggest absorbed energy occurs at lowest strain rates therefore the standard tensile test results must be considered for structural designs.

Figure 31- Sikadur 330 strain rate behavior.

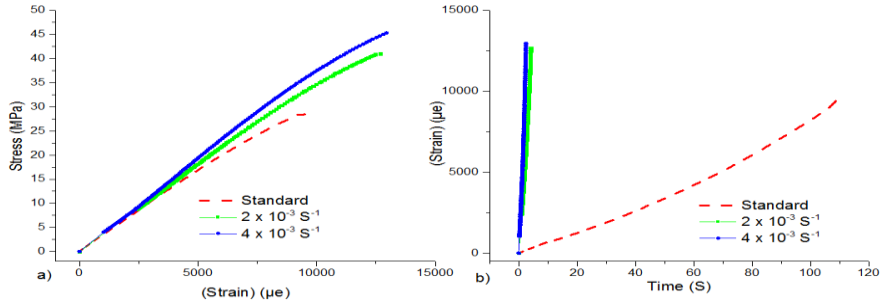

Figure a: Stress-Strain curves relationship. Figure b: Strain-Time curves relationship.

Note: 1000 (με) =0.001 absolute strain.

Figure 32 - Sikadur330 strain rate behavior vs standard tensile test behavior.

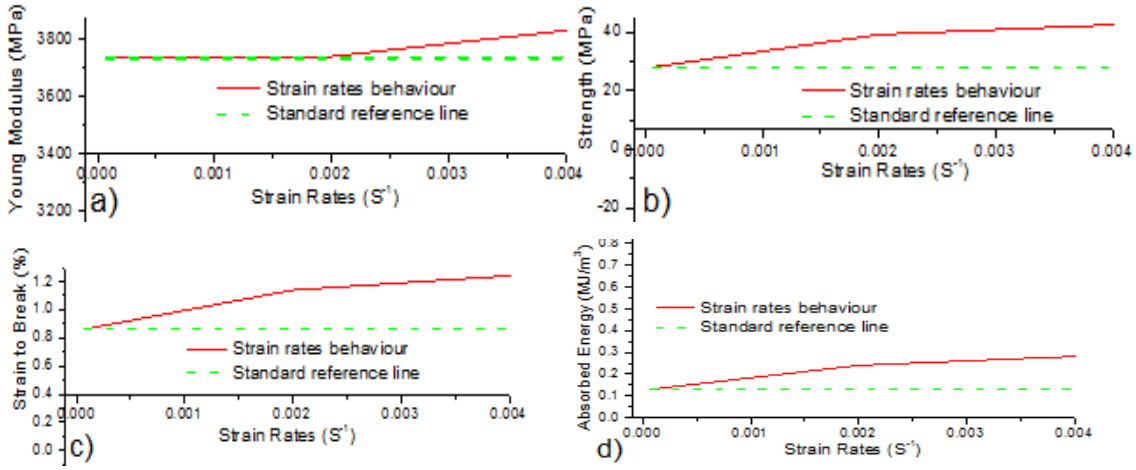

a) Young modulus vs Strain rates curve. b) Tensile strength vs Strain rates curve. c) Strain to break vs Strain rates curve. d) Absorbed energy vs Strain rates curve.

5.4.4 Strain rates discussion

Mechanical properties of Sikacarbodur S512 and adhesives bonding materials show different behavior when analyzed at different strain rates compared with standard tensile test behavior. Sikacarbodur S512 Young modulus decreased 12% when strain rates increase whereas Sikadur30 Young modulus decreased 10% and Sikadur330 Young modulus is strain rate insensitive. Sikacarbodur S512 and sikadur 30 tensile strength are strain rate insensitive whereas Sikadur 330 tensile strength increased 45%. Sikacarbodurs512 strain to break increased 15% and Sikadur 330 strain to break increased 40% whereas; sikadur30 strain to break is strain to rate insensitive. Sikacarbodur S512 and Sikadur 30 absorbed energy are strain

rate insensitive whereas Sikadur 330 absorbed energy increased 100%. For structural design, it is recommended to neglect the enhancement of mechanical properties under strain rates dependent behavior, which their upper limit is defined by standard tensile test results because those increments occur in a very short time before failure.

The results shows that under different strain rates, mechanical properties of materials are increased, meaning that the materials are strain rate dependent although those increments in mechanical properties for structural design is better to be considered as an additional safety factor for the materials performance. Besides considering that the failure modes are kept into a brittle behavior thus, the strain rate dependency for the studied materials is not as useful as desired.

When compared the results with literature where other research groups considered highest strain rates the obtained results for SikacarbodurS512 match very well. Shimet et.al[7] observed in carbon fiber filled liquid crystalline polymer composite Vectra A230 that the strain to break and Young modulus are strain rate sensitive. Daniel et.al[8] observed in unidirectional plate SP288/AS graphite/epoxy that the Young modulus is strain rate sensitive whereas tensile strength is strain rate insensitive. However, the results did not match for tensile strain to break where he observed strain rate insensitive behavior. Harding[5] observed that in unidirectional reinforced carbon/epoxy plate the tensile strength is strain rate insensitive. However, the results did not match for Young modulus where he observed a strain rate insensitive behavior. Chamis CC et.al[9] observed that in carbon/epoxy composite the Young modulus is strain rate sensitive whereas the tensile strength is strain rate insensitive, these results match very well with the obtained result in this research. This research considered the strain rate behavior defined correlated to standard tensile test results because are those results, which are shown in manufacturer datasheets, and are those ones considered every time that a structural design is performed.

6 MICROGRAPH ANALYSIS

6.1 CFRP micrograph analysis

SEM micrograph analysis before tensile tests shows the longitudinal distribution of fibers in lamina sikacabodur S512 (Figure 33).The fiber diameter remains constant all over the length of the plate also the resin layer changes in thickness because this one depends on fibers and resin arrangements which is a random arrangement depending of pultruded manufacturing process. Some longitudinal fibers discontinuities and misalignments were found, and this may influence some mechanical properties differences on tensile tests.

In the cross-section image, it is observed that fibers are close packaged. The resin is covering the fibers, although some localized cracks and bubbles can be observed. This effect may be attributed either to the processing of material or the SEM sample preparation, however regarding Figure 33 (a, b) where fiber discontinuities (shown by arrows) and fiber misalignments (shown by line AB) are observed, these defects could not be provoked by SEM samples preparation. Perhaps some fibers discontinuities (but not all of them) might be caused while CFRP plate transportation, considering that an external side of the fiber in Figure 33 (a, b) is analyzed. However, fiber misalignments in the same figure (shown by line AB) could not be provoked while CFRP plate transportation. Moreover observing Figure 33c some carbon fiber and interfacial cracks are found (shown by arrows), whereas a Figure 33d is showing a cross section without cracks in carbon fibers. Therefore, it is noticed that fiber discontinuities and fiber misalignments are neither provoked while SEM samples preparation nor CFRP plate transportation but while CFRP plate manufacturing.

Figure 33 - SEM image of longitudinal direction of Sikacarbodur S512 material.

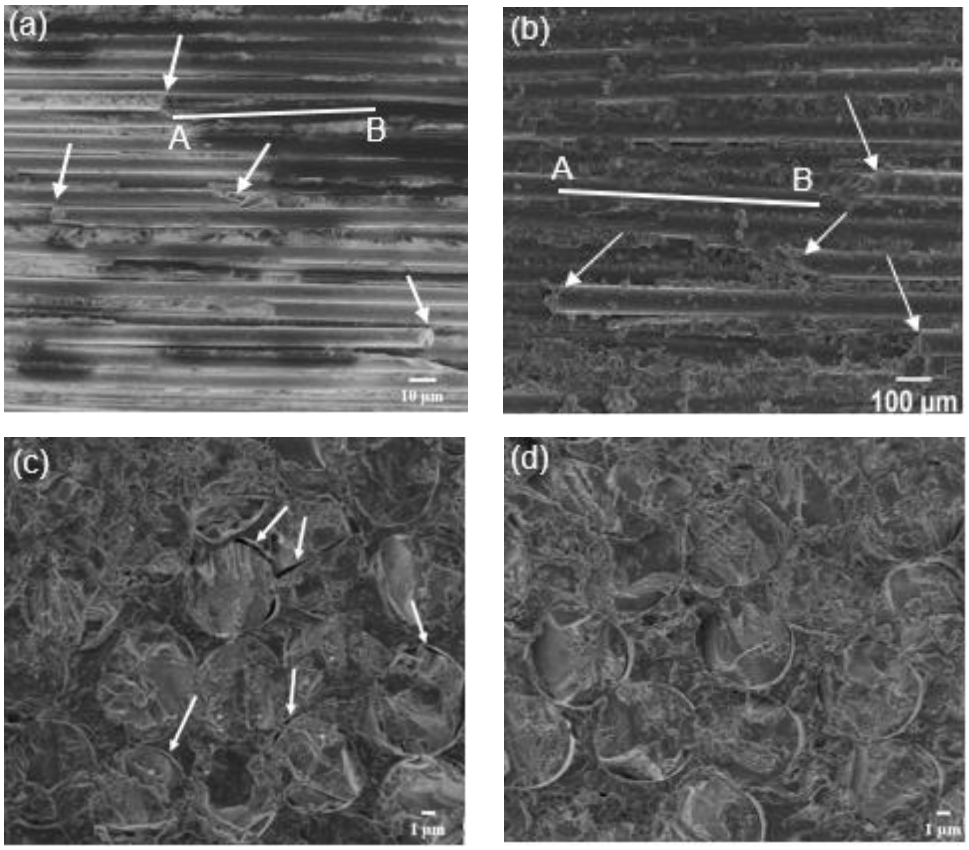

Figure (a, b) SEM image of longitudinal direction of Sikacarbodur S512 material. (c) SEM cross-section image of Sikacarbodur S512 material. (d) SEM cross-section image of Sikacarbodur S512 material before tensile tests

6.1.1 Carbon fiber volume fraction on Sikacarbodur S512

To determinate the carbon fiber volume fraction, first was calculated the carbon fiber diameter using Image J free software. Figure 34 shows the frequency and the diameter measurements as well as the SEM image of carbon Fiber volume fraction, indicating that the average of the carbon fiber diameter of Sikacarbodur S512 material is 6.7 µm. The average of the carbon fiber diameter, the volume fraction of resin and Carbon fiber in Sikacarbodur S512 were calculated as shown in Table 17. The result shows a volume fraction of carbon fiber around 63 % and 37 % for resin, which means that Sikacarbodur S512 has enough carbon fiber volume to assure the maximum mechanical properties at lowest cost.

Figure 34 - SEM image of carbon Fiber diameter distribution.

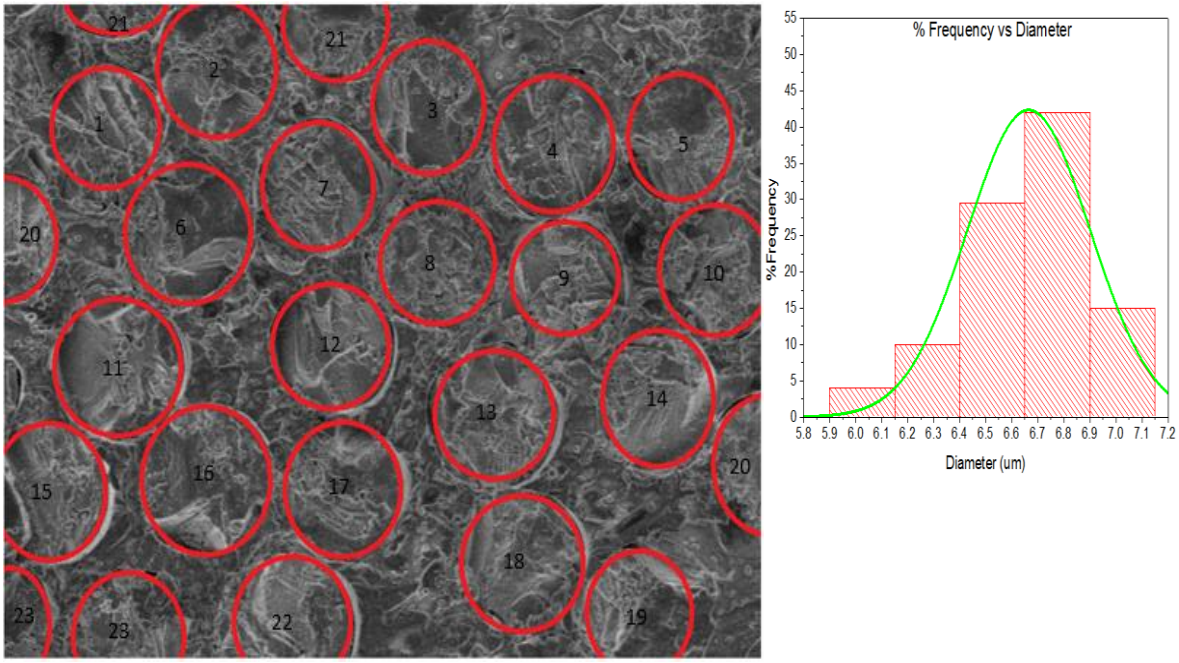

Table 17 - Carbon fiber volume fraction.

Composite area	1266.52	(µm)^2
Fiber diameter	6.663	µm
Total of fibers	23	units
Total area of fibers	801.97	(µm)^2
Fiber volume fraction	63.32	%
Resin volume fraction	36.68	%

6.1.2 Carbon Fiber Standard Tensile Test Failures Surfaces

Figure 35 shows Sikacarbodur S512 before and after mechanical tests, and the figure shows a failure surface typically of a brittle material where failure occurs of a suddenly way. Figure 36 presents SEM micrograph analysis showing that the fiber failure surface is non-planar and irregular with serrated aspect, besides a resin debris due to matrix debonding was observed. However, adhesive fracture was the predominated failure mode. It is important to notice that no shrinkage in diameter was observed after tests, proving that fibers have a brittle fracture. Figure 37 shows the interfacial crack propagation before matrix debonding. The matrix does not transfer in a uniform way all the forces among fibers, and some interfacial cracks are avoiding the force to be transferred in a properly way. Figure 38 shows matrix debonding which is a process following the interfacial crack propagation.

SEM micrograph analysis shows rough surfaces after test (Figure 39). Moreover shows that the failure direction is perpendicular to a fiber and load direction. The surface after test is non-planar and irregular; also, some carbon fiber failures are consequence of fiber manufacturing defects (shown in Figure 33) as misalignments, discontinuities and cracks in fiber surface.

Figure 35 - SEM image of Sikacarbodur S512 before and after tensile test.

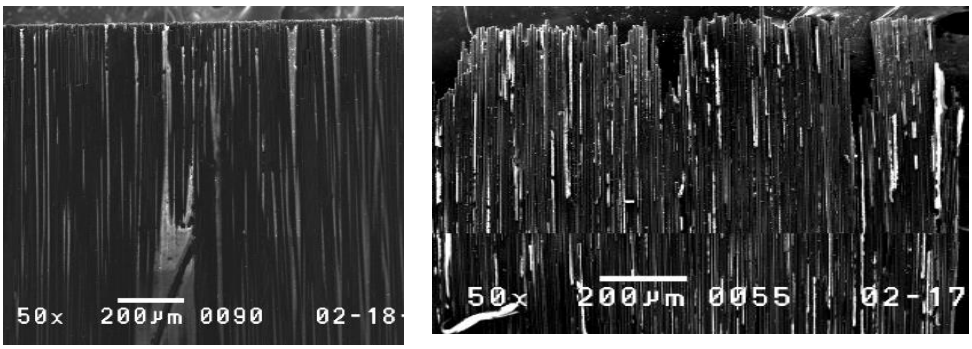

Figure 36 - SEM image of carbon fiber failure surfaces

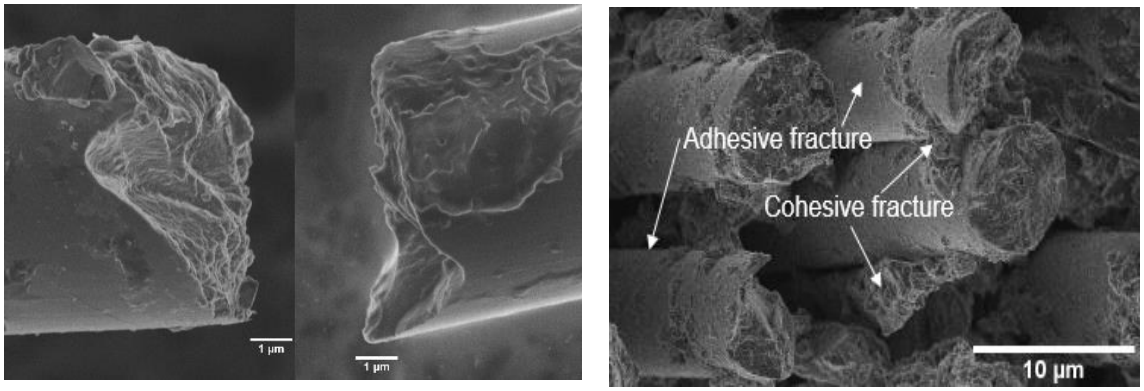

Figure 37- SEM image of interfacial crack propagation.

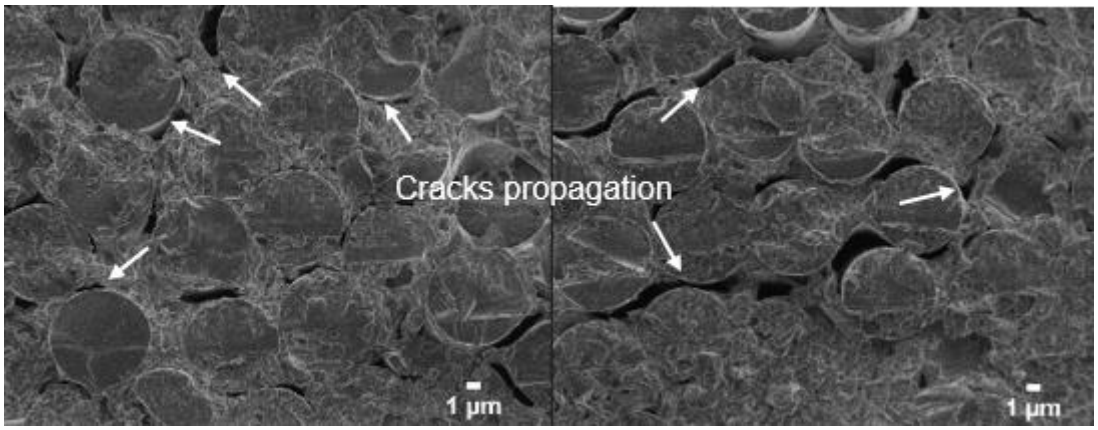

Figure 38 - SEM image of Matrix debonding.

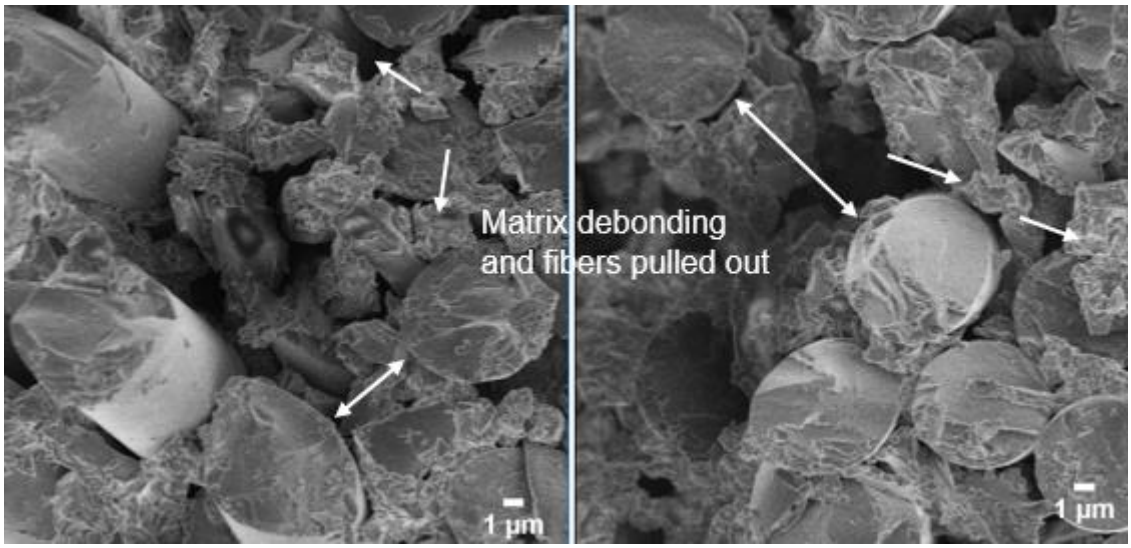

Figure 39 - SEM image of carbon fiber failed cross sections.

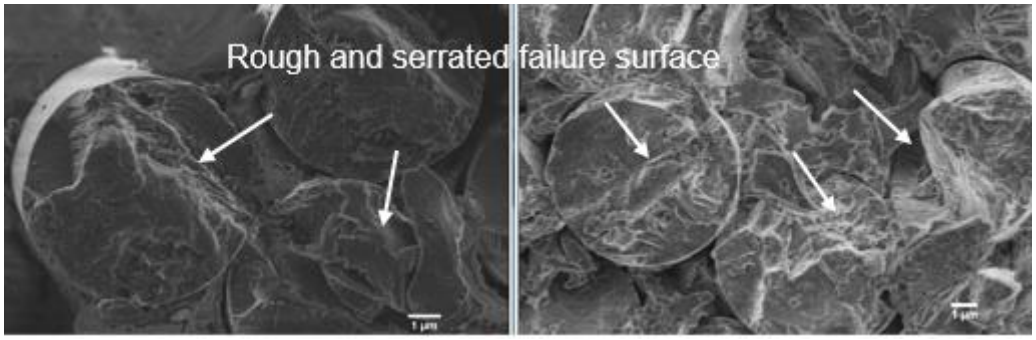

As shown in Figure 37 and Figure 38 describing the sequence of failure of carbon fiber starting by the interfacial crack propagation, the interfacial cracks can avoid the force to be transferred in a properly way, generating a matrix debonding, which finally pull out carbon fibers. Moreover, a fiber-matrix interphase failure mode is observed due to tensile stress concentration in fiber-matrix interphase for glass fibers [(14)]. Matrix among fibers are restricted to be deformed by covalent alloys between matrix and fibers and once fibers started to be deformed, the local stress in matrix increased, however covalent alloys between matrix to matrix are stronger than covalent alloys between fiber to matrix. Regarding the failure observed, Sikacarbodur S512 plate is not a ductile material and its matrix cannot transfer properly the force among fibers due to cracks propagations and tensile stress concentrations in fiber-matrix interphase.

To enhance the adhesion between fibers and epoxy resin Mohammed [15] used sizing agent of carbon nanotube (CNT) in carbon fiber or in neat epoxy resin and he observed that the sizing agent improved the load carrying capacity and toughness of RC columns confined with carbon fiber/epoxy composites. Hongwei [16] concluded that using novalac resin in the fiber sizing has proved to be the most effective way to increase the carbon fiber epoxy resin bonding. Nevertheless many researchers [24,18, 2] observed that when fastening CFRP to a steel element the failure is in the adhesive-steel interface. The failure mode when strengthen a concrete beam could be shear failure, flexural failure and FRP debonding [25,17] . Therefore, when using FRP as retrofitting materials the failure occurs in the interface zone or a cohesive fracture mode defined by concrete failure whereas the FRP remains without damage, this is indicating that to enhance the adhesion between fiber and epoxy resin in a composite material will depend on the specific application which is needed.

6.2 Sikadur 30 micrograph analysis

Figure 40a shows a backscattered electron image (BSE) of sikadur 30 cross section without carbon coating where it is possible to identify two different phases a dark and continuos phase and a bright granular phase: Figure 40b (region 1) shows a predominated granular phase which reject more electrons, that is way this region seems to be less dark.. Figure 40c (region 2) shows a predominated continuous phase this region catches some electrons and does not reject as much electrons as region 1, that is way it looks a little bit dark. When a carbon coating is used the differences between regions disappears, thus both regions reject similar amount of electrons. Figure 40d shows the interfacial phase (located in the interception zone between granular phase and continuous phase). Moreover observing Figure 40¨b¨,¨c¨ and ¨d¨ is found that sikadur 30 presents a porous surface which is the reason of the brittle behavior. Force transferring is affected and the material is not able to develop a necking behavior by diffusing its cross section. Some defects are observed in the cross section; those ones are due to trapped air bubble during the samples preparing procedure and could be avoided if a vacuum environment system is settle during the preparing procedure. However regarding that during the application of the material in any retrofitting project is not common the used of any vacuum system, those defects were considered as a normal consequence of the procedure followed to prepare the samples, and mechanical properties must be determined considering them.

Figure 40 - SEM image of Sikadur 30 cross-section surface before tensile test.

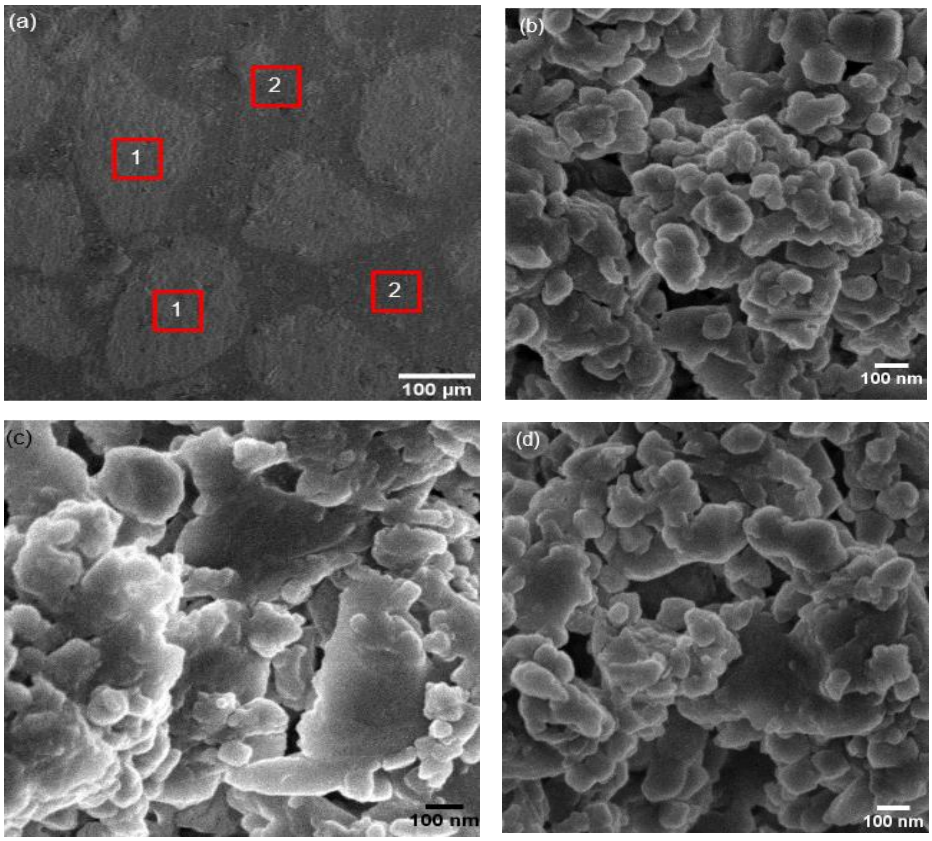

Figure a: SEM image of Sikadur 30 cross-section surface before tensile test without carbon coating. Figure b: Predominated granular phase, magnified image of region 1. Figure c: Predominated continuous phase, magnified image of region 2. Figure d: Interfacial phase between regions.

Sikadur 30 micrograph analysis after tensile test

Figure 41 shows a rough, irregular and nonplanar surface typically of brittle materials, and there are many granular particles over the continuous phase of the resin inside the curve inward of a concave surface. Figure 41b is a high magnification image of region 1 and it shows that the curve inward of concave surfaces are composed by a continuous phase of the resin coated by fine granular particles. Figure 41c shows a mixing between fine granular particles and continuous phase of the resin found in region 2. Figure 41d (region 3) shows that there is a part of the cross section in the cast where is composed just by the continuous phase of the resin. Before tensile test, there was a part in the cast cross section governed by fine granular particles (Figure 40, b) but after the tensile tests, the surface became rough and irregular, that part was mixed with a continuous phase of the resin and became what is observed in Figure 41 (b and c). The continuous phase remains constant but some cracks are shown as consequence of strength concentration.

Crosslinking of the adhesive itself is one of the factor used to measure the adhesive efficiency. Here the crosslinking performance is described as follow: The failure procedure started in region 3, where some groove are shown without fine granular particles this is indicating that covalent alloys between fine granular particles and the continuous phase were broken therefore fine granular particle were expelled. Simultaneously failure was occurring in region 1, here it is observed the continuous phase coated by fine granular particles but the continuous phase is not concentrated as it was before tensile test, indicating that covalent alloys inside the continuous phase were broken. Therefore, in this region part of the continuous phase was expelled. Then region 2 was less affected than the other regions however, some cracks are also observed indicating that it was reached by the subjected stress.

Figure 41- SEM image of Sikadur 30 sample after tensile test.

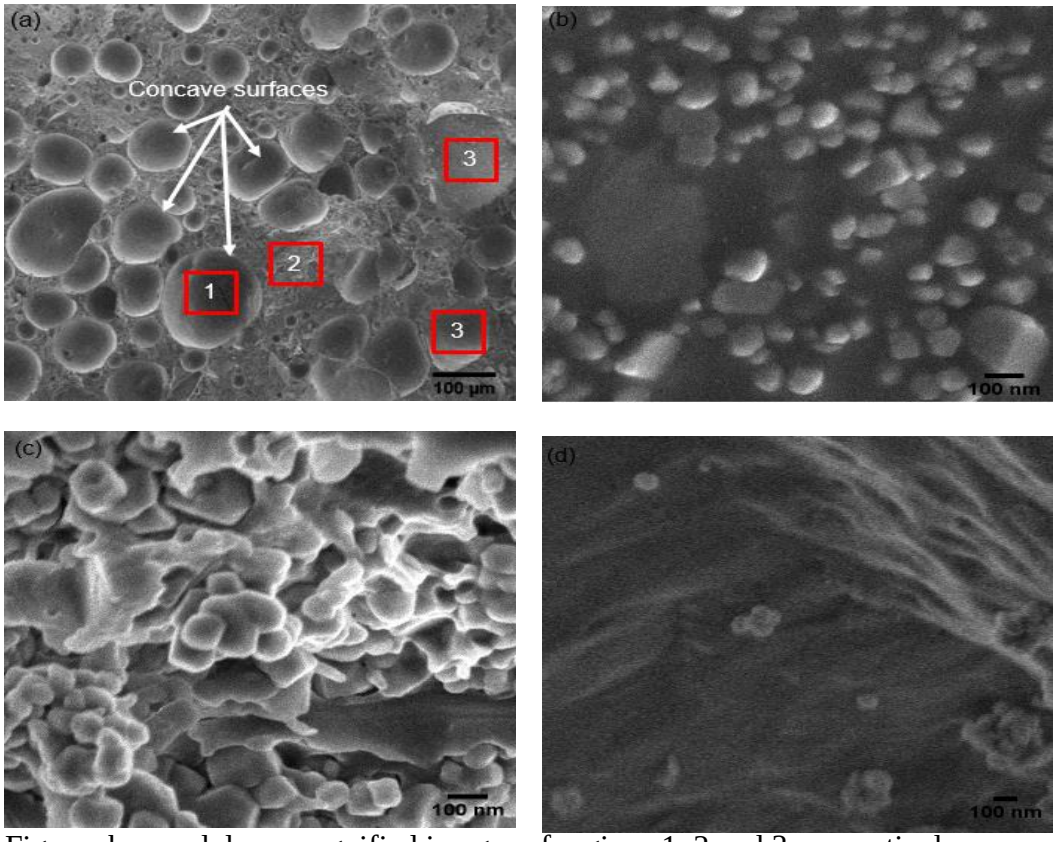

Figures b, c and d are magnified images of regions 1, 2 and 3, respectively.

6.3 Sikadur 330 micrograph analysis

Figure 42 shows that sikadur 330 has a homogenous distribution of phases the granular and the continuous phase are scattered in a uniform way as observed in Figure 42a , which assures that the fine granular particles are coating the continuous phase of the resin for Sikadur 330 material. Moreover, it is observed that sikadur 330 has a porous surface, which leads to have a brittle behavior avoiding the diffusing of its cross section during tensile test.

Figure 42 - Typical SEM image of Sikadur 330 cross-section surface before the tensile test.

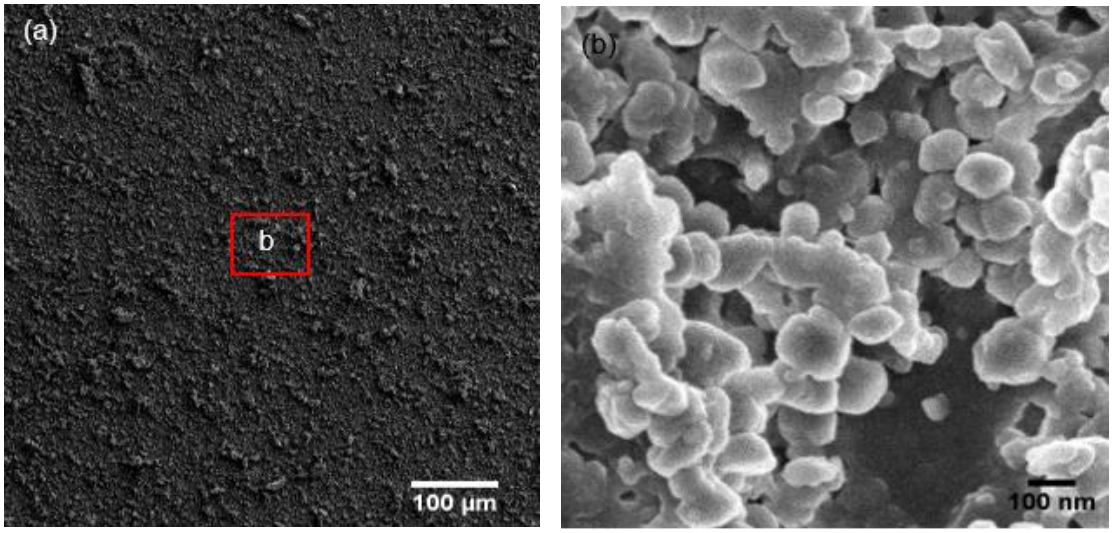

Sikadur 330 micrograph analysis after tensile test

Figure 43a shows some micro cracks (red arrows) propagation in the continuous phase surrounding the granular phase which is outspread all over the curve inwards of the concave surface (Figure 43d). Figure 43b (region 1) shows after tensile test the fine granular phase of the resin scattered all over the continuous phase in the curve inwards of the concave surface, they are not as concentrated as they were before tensile test. However, as shown in Figure 43c (region 2) some parts in the cross section remained with a homogenous distribution as they were before tensile test, which means that the applied force distribution was not able to affect that part of the cross section before failing. It is observed that sikadur 330 has less concave surfaces than sikadur 30; this means that sikadur 330 develops more deformations before its covalent alloys start to break.

Sikadur 330 crosslinking performance is indicating that in region 1, covalent alloys inside the continuous phase were broken because fine granular particles are observed, cracks outside region 1 indicates the zones of stress concentration. Region 2 was not affected as region 1

nevertheless; region 2 addressed the stress distribution to the most critical zone. In this material, it was not observed any region where covalent alloys between fine granular particles and continuous phase were broken. Thus, covalent alloys inside continuous phase of sikadur 330 are stronger than covalent alloys of sikadur 30; consequently, sikadur 330 has bigger strain to break than sikadur 30 and a bigger capacity to absorb energy, although they have similar tensile strength.

The results obtained from the detailed study correlating mechanical properties with scanning electron microscopy analysis of sikacarbodur S512, sikadur 30 and sikadur 330 materials enabled us to understand deeply the critical aspects of applying composites and resins in practical. Besides, it shows the importance of using advanced techniques of characterization, like SEM, to understand better the mechanical properties. Certainly, similar approach can be used for other materials in civil engineering.

Figure 43 - SEM image of Sikadur 330 cross-section surface after tensile test.

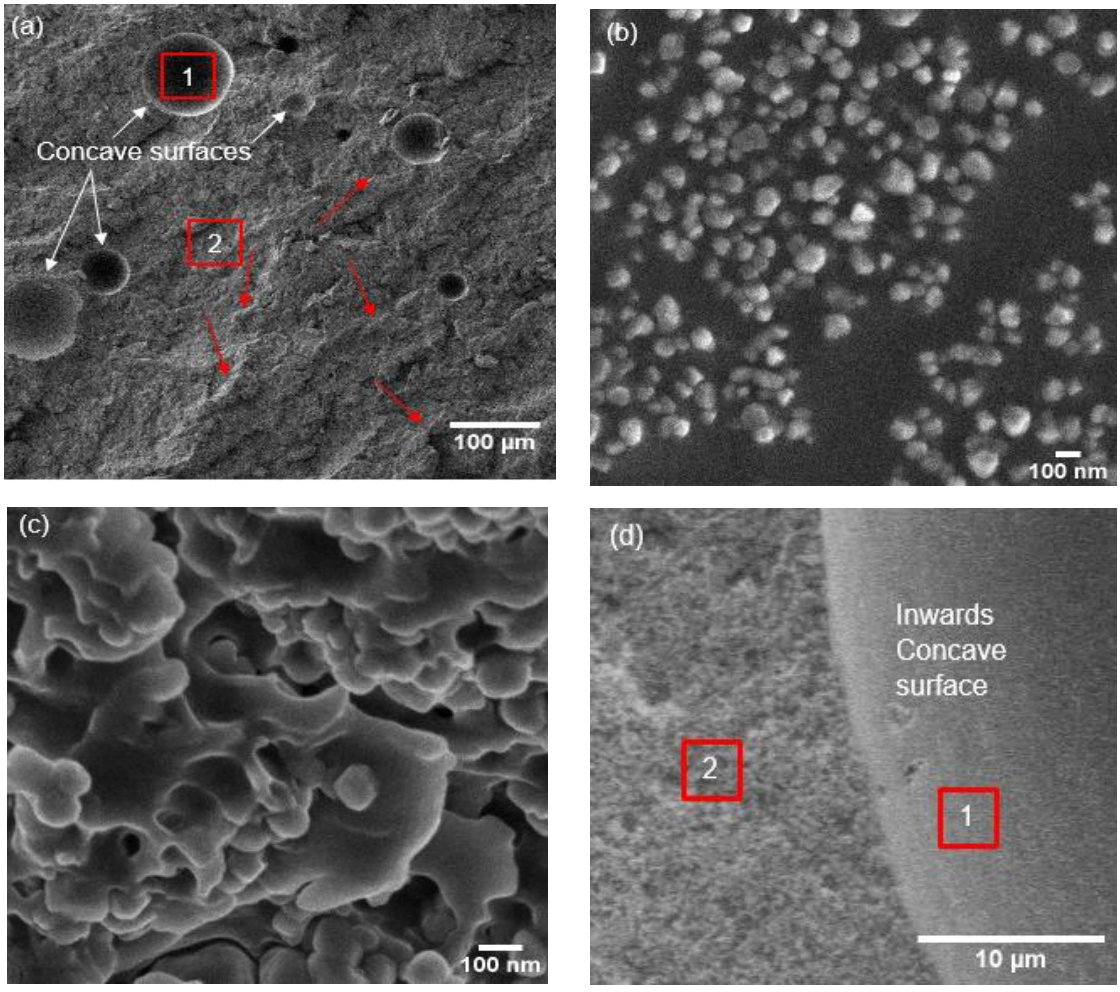

Figure b and c are magnified images of region 1 and 2, respectively. Figure d is the interface between region 1 and region 2.

7 CONCLUSIONS AND RECOMMENDATIONS

In this research, tensile tests for Sikacarbodur S512 and Sikadur 30 following ASTM D3039/D3039M and ASTM D638-14 respectively were used to evaluate the strain rate dependent behavior of composite materials and epoxy.

After analyzing stress-strain curves of Sikacarbodur S512 obtained at room temperature with a standard head displacement rate of 2 mm/min, it was found that Sikacarbodur S512 does not have ductile behavior and it is not able to sustain inelastic deformation since an elastic range governs its mechanical performance. Therefore, special cares must considered when recommending Sikacarbodur S512 as retrofitting or reinforcement material for elements in areas under high seismic hazards.

Sikadur 30 and Sikadur 330 stress-strain curves show that the epoxies adhesive do not have any significant plastic range and a nonlinear elastic range governs their main mechanical behavior under tensile loads. Moreover, their yielding stress is not clearly defined. When comparing stress-strain behavior of sikadur 30 and sikadur 330 it is noticed that, sikadur 330 has better seismic behavior than sikadur 30 since both have almost the same tensile strength but sikadur 330 has the biggest strain to break, more than twice. Therefore, Sikadur 330 has better capacity to absorb energy.

Mechanical properties of Sikacarbodur S512 and adhesives bonding materials show different behavior when analyzed at different strain rates compared with standard tensile test behavior. Sikacarbodur S512 Young modulus and Sikadur 30 Young modulus are strain rates dependent whereas Sikadur330 Young modulus is strain rates independent. Sikacarbodur S512 and Sikadur 30 tensile strength are strain rates independent whereas Sikadur 330 tensile strength is strain rates dependent. Sikacarbodurs512 and Sikadur 330 strain to break are strain rates dependent, whereas Sikadur 30 strain to break is strain rates independent. Sikacarbodur S512 and Sikadur 30 absorbed energy are strain rates independent whereas Sikadur 330 absorbed energy is strain rates dependent. Therefore, the studied materials have a strain rates dependent behavior. For structural design, it is recommended to neglect the increments in mechanical properties when strain rates are increased. Results of mechanical properties under standard tensile test must be used for structural designs.

Sikacarbodur S512 micrograph analysis shows that the fracture behavior is addressed by the interphase zone (contact zone between fiber and resin) which is affected by tensile stress concentration and cracks propagations. Fiber-matrix interphase failure mode occurs after covalent alloys are broken due to tensile stress concentration in fiber-matrix interphase, affecting the load transferring to carbon fibers. Thus, matrix debonding occurs and finally carbon fibers are pulled out, that is because Sikacarbodur S512 plate is not a ductile material and its matrix cannot transfer properly the force among fibers.

Micrograph analysis before and after tensile test of Sikadur 30 and Sikadur 330 shows that they have a continuous phase and a granular phase. In both resins covalent alloys are broken, however sikadur 30 showed the most critical behavior because its fine granular particles are expelled out whereas sikadur 330 remained with its fine particles linked to its continuous phase after tensile test. This is indicating that sikadur 330 has better mechanical behavior under uniaxial tensile test than sikadur 30, that better behavior is understood when their tensile strain to break and absorbed energy capacity are compared. In general, failure surfaces are perpendicular to the applied force. Moreover, sikadur 330 has a better cross section distribution than sikadur 30.

8 FUTURE WORKS

For future work is highly recommended to evaluate strain rate dependent behavior influence in Poisson ratio.

To use at least five-crosshead stroke rate considering slower speed than the maximum considered in this research. This because for epoxy adhesive, it was found to have few experimental data (just from tensile test at two different crosshead stroke rates) to compared with standard tensile test results, therefore to re-evaluate the strain rate dependent behavior is required.

To develop a micromechanical method for these materials to characterize its mechanical behavior under different strain rates and different loading conditions is encouraged.

REFERENCES

1 SHOKRIEH, M. M.; OMIDI, M. J. Tension behavior of unidirectional glass/epoxy composites under different strain rates. **Composite Structures**, v. 88, p. 595-601, 2009.

2 ABED, G. M. H. **Effects of temperature on the adhesive bonding in steel beams reinforced with CFRP composites**. 2012. 208 p. Thesis (Doctor of Philosophy) - Faculty of Engineering and the Environment, University of Southampton, Southampton, 2012.

3 MICHELS, J.; WIDMANN, R.; CZADERSKI, C.; ALLAHVIRDIZADEH, R.; MOTAVALLI, M. Glass transition evaluation of commercially available epoxy resins used for civil engineering applications. **Composites Part B**, v. 77, p. 484-493, 2015.

4 McNUTT, J. N. **Damage repair of bridge superstructures using bonded composite patching**. 2011. 373 p. Thesis (Master of Science) - Faculty of the Graduate School, Vanderbilt University, Nashville, 2011.

5 HARDING, J.; WELSH L. M. A tensile testing technique for fiber-reinforced composites at impact rates of strain. **Journal of Material Science**, v. 18, n. 6, p. 1810-1826, 1983.

6 WELSH, L. M.; HARDING, J. Effect of strain rate on the tensile failure of woven reinforced polyester resin composites. **Journal de Physique Colloques**, v. 46, n. 6, p. 405-414, 1985.

7 SHIM, V. P. W.; YUAN, J.; LIM, C. T. Dynamic tensile response of a carbon fiber reinforced LCP composite and its temperature sensitivity. **Proceedings of SPIE**: the International Society for Optical Engineering, v. 4317, p. 100-105, 2001.

8 DANIEL, I. M.; LABEDZ, R. H.; LIBER, T. New method for testing composites at very high strain rates. **Experimental Mechanics**, v. 21, n. 2, p. 71-77, 1981.

9 CHAMIS, C. C.; SMITH, G. T. Environmental and high strain rate effects on composites for engine application. **American Institute of Aeronautics and Astronautics Journal**, v. 22, n. 1, p. 128-134, 1984.

10 GILCHRIST, M. D.; SVENSSON, N. A fractographic analysis of delamination within multidirectional carbon/epoxy laminates. **Composites Science and Technology**, v. 55, p. 195-207, 1995.

11 ARASH, A.; MAEN, A.; CHAD, S. K; FU-PEN, C. Effect of long-term exposure to marine environments on the flexural properties of carbon fiber vinylester composites. **Composite Structures**, v. 126, p. 72-77, 2015.

12 CHENG, L.; DANDAN, D.; HUAGAN, L.; YUBING, H.; YIWEI, X.; JINGMING, T.; GANG, T.; JIE, T. Interlaminar failure behavior of GLARE laminates under short-beam three-point-bending load. **Composites Part B**, v. 97, p. 361-367, 2016.

13 ALBEDAH, A.; SOHAIL, M. A. K.; BENYAHIA, F.; BOUIADJRA, B. B. Effect of load amplitude change on the fatigue life of cracked Al plate repaired with composite patch. **International Journal of Fatigue**, v. 88, p. 1-9, 2016.

14 HORST, J. J.; SPOORMAKER, J. L. Fatigue fracture mechanisms and fractography of short-glassfibre-reinforced polyamide 6. **Journal of Materials Science**, v. 32, p. 3641-3651, 1997.

15 MOHAMMAD, I. R.; MOHAMMED, A. H.; MAHMOUD, A. Using carbon nanotubes to improve strengthening efficiency of carbon fiber/epoxy composites confined RC columns. **Composite Structures**, v. 134, p. 523-532, 2015.

16 HONGWEI, H.; KAIXI, L.; FENG, G. Improvement of the bonding between carbon fibers and an epoxy matrix using a simple sizing process with a novolac resin. **Construction and Building Materials**, v. 116, p. 87-92, 2016.

17 MOHAMMAD, I. R.; MOHAMMED, A. H.; MAHMOUD, A. Effect of using carbon nanotube modified epoxy on bond-slip behavior between concrete and FRP sheets. **Construction and Building Materials**, v. 105, p. 511-518, 2016.

18 KIM, Y. J.; HARRIES, K. A. Fatigue behavior of damaged steel beams repaired with CFRP strips. **Engineering Structures**, v. 33, p. 1491-1502, 2011.

19 TÄLJSTEN, B.; HANSEN, C. S.; SCHMIDT, J. W. Strengthening of old metallic structures in fatigue with prestressed and non-prestressed CFRP laminates. **Construction and Building Materials**, v. 23, p. 1665-1677, 2009.

20 MERTZ, D. R.; GILLESPIE, J. W.; CHAJES, M. J.; SABOL, S. A. **Rehabilitation of steel bridge girders through the application of advanced composite materials**. Washington, DC: IDEA, 1996. 35 p. project final report, contract NCHRP-93-ID011.

21 GHAFOORI, E.; MOTAVALLI, M.; BOTSIS, J.; HERWIG, A.; HERWIG, A.; GALLI, M. Fatigue strengthening of damaged metallic beams using pretressed unbonded and bonded CFRP plates. **International Journal of Fatigue**, v. 44, p. 303-315, 2012.

22 MIRMIRAN, A.; SHAHAWY, M. Behavior of concrete columns confined by fiber composites. **Journal of Structural Engineering**, v. 123, n. 5, p. 583-590, May 1997.

23 DONG, J. F.; WANG, Q. Y.; CUAN, Z. W. Structural behavior of RC beams externally strengthened with FRP sheets under fatigue and monotonic loading. **Engineering Structures**, v. 41, p. 24-33, 2012.

24 MASSIMILIANO, B.; PIERLUIGI, C.; GIULIA, F.; CARLO, P. Interaction of interface delamination and plasticity in tensile steel members reinforced by CFRP plates. **International Journal of Fracture**, v. 146, p. 79-92, 2007.

25 ARAM, M. R.; CZADERSKI, C.; MOTAVALLI, M. Debonding failure modes of flexural FRP-strengthened RC beams. **Composites Part B**, v. 39, p. 826-841, 2008.

26 GOTRO, J. The winding road to renewable thermoset polymers part 5: epoxies. In: INNOCENTRIX. **Polymer innovation blog**. 2013. Available in: <https://polymerinnovationblog.com/the-winding-road-to-renewable-thermoset-polymers-part-5-epoxies/>. Access in: 10 abr. 2017.

27 POCKET DENTISTRY. **Dental polymers**. 2015. Available in: <http://pocketdentistry.com/dental-polymers-2/ >. Access in: 10 Apr. 2017.

28 PENNSYLVANIA STATE UNIVERSITY. Penn State Department of Chemistry. **Polymers chemistry 112**: supplementary reading. 2013. Available in: <http://courses.chem.psu.edu/chem112/materials/polymers.html>. Access in: 10 Apr. 2017.

29 CAMPBELL, F.C. **Structural composite materials**. Ohio: ASM International, 2010. 612 p.